CHALMERS

Influence of Support Stiffness in Dynamic Analysis of Piping Systems

Master's Thesis in Solid and Fluid Mechanics

JESPER AXELSSON
HENRIK VIKTORSSON

Influence of Support Stiffness in Dynamic Analysis of Piping Systems

Master's Thesis in Solid and Fluid Mechanics

JESPER AXELSSON
HENRIK VIKTORSSON

Influence of Support Stiffness in Dynamic Analysis of Piping Systems
JESPER AXELSSON
HENRIK VIKTORSSON

Cover:
Mesh of typical piping system.

Influence of Support Stiffness in Dynamic Analysis of Piping Systems
Master's Thesis in Solid and Fluid Mechanics
JESPER AXELSSON
HENRIK VIKTORSSON
Department of Applied Mechanics
Division of Dynamics
Chalmers University of Technology

Abstract

Reliable finite element analyses and simulations of nuclear power plant piping systems are extremely important for obvious reasons. According to regulations and norms the finite element analyses are to be carried out rigorously. One delicate task is how to model the gaps between the piping systems and the supports. Gaps often give rise to large accelerations when closed. This results in large forces according Newtons second law. These forces have a very short duration and their influence on the structure is difficult to determine. Today, gaps up to 5 mm are commonly neglected although the effects on stresses and forces are not well known. The aim of this thesis is to estimate the influence of the gaps and to study the effect of different support stiffnesses combined with gaps.

Two piping systems are investigated, one simple geometry with two supports that resembles a main steam system and one typical main steam system with a more complex geometry containing more supports. Both systems are modeled with supports that contain gaps. The systems are modeled using the, for piping systems, specialized finite element code Pipestress and the general purpose code ANSYS. Almost exclusively in Swedish nuclear power plant industry Pipestress is used although it lacks the possibility to model gaps. ANSYS has the possibility to model the gaps. The resulting nonlinear contact problems are solved using Lagrange multiplier method in the normal direction while the Penalty method is used in the tangential direction.

A wide span of gaps, from 0 - 800 mm, are considered. The load case considered is the transient of a pipe break load. The resulting support contact forces are a local phenomenon and do not have a visual effect on the pipe stresses. Though, all effects are not completely known. With this in mind, the conclusion is made that it is a reasonable approximation to neglect gaps up to 5 mm if the reaction force spikes are neglected. Larger gaps can also be simplified to no gap if reaction forces may be neglected. However, these forces may be very large and if local effects are of great importance they need to be taken into account.

Keywords: Piping systems, Pipe support, Dynamic analysis, Non linear pipe support

Contents

Preface

In this investigation the influence of gaps between a pipe and its supports in piping systems has been investigated. Finite element analyses have been performed to investigate if approximations, imposed by the industry, regarding gaps in supports are accurate. The work has been performed from January 2011 to June 2011, at the Department of Applied Mechanics, Division of Dynamics, Chalmers University of Technology, Sweden, and the Department of Nuclear Engineering, Epsilon Development Center Väst AB, Sweden, with Professor Mikael Enelund as examiner, M.Sc John Lennby as supervisor and M.Sc Robert Magnusson as supervisor.

Aknowledgements

We would like to thank our examiner and our supervisors, for the support and thanks also to M.Sc Emil Carlsson manager at the Department of Nuclear Engineering, Epsilon Development Center Vast AB, Sweden.

Göteborg June 2011
Jesper Axelsson, Henrik Viktorsson

1 Introduction

Due to high demands on safety and structural integrity, all pipes in Swedish nuclear power plants have to be analyzed and approved according to the ASME code [3]. This is normally done with the finite element analysis software Pipestress [4]. Pipestress is specialized for piping systems and is used because of its simplicity and the fact that it evaluates stresses directly against the ASME code. A drawback to Pipestress is that it can not model pipe supports with nonlinear stiffnesses, for example, gaps. The research in this area is limited and the effects of nonlinear gap stiffness are not well known. This is what this thesis is aimed to investigate.

1.1 Background

All piping systems at Ringhals nuclear power plant and other Swedish nuclear power plants are regulated by nationals laws and regulations and, more specifically, by the ASME boiler and pressure vessel code section III. The ASME code contains information such as allowable material stress values and governing stress equations. According to this, all piping systems are divided into five safety classes, 1, 2, 3, 4 and 4a, where class 1 pipes (usually close to the reactor) have the highest demands on structural integrity and class 4 pipes have the lowest. This classification is, by tradition, based on American laws and norms. Service levels are also defined by the ASME code. They are, in order of decreasing likelihood of occurrence and increasing severity, levels, A(normal), B(upset), C(emergency) and D(faulted). Typical level A loadings are those occurring during normal conditions such as operating pressure and dead weight. Level B loads occur occasionally but should not cause any damage requiring repair, for example, fluid hammers due to valve closure or relief valve discharge, see Section 2.6. A level C load is usually severe enough to cause large deformations. A level D load is the most unlikely to occur and only does so under extreme conditions, for example, an earthquake or a main steam pipe break.

There are several different types of pipe supports that are used in nuclear power plants. The type that is used in a specific case depends on the expected loadings and boundary conditions. According to [13], the four most commonly used support types are:

1. Weight supports
   Only used to compensate the vertical dead weight load of a pipe. Below are some examples.

   - Rod hangers
     A rod hanger is a rigid support that works well in tension but not in compressions. It is therefore always placed above the pipe. It should only be used on pipes where thermal movement is low, otherwise there is a risk of thermal lockup which can lead to expansion overstress in the pipe.

   - Sliding supports
     If there is no space above the pipe or nothing to attach a hanger to, a sliding support can be used. It is a rigid support that the pipe can rest on but also allows sliding in the horizontal direction. It does not support the pipe in the upward direction and should not be used if there is risk of large upward forces.

   - Spring hangers
     In cases where the thermal movement is high, the two previous rigid supports

can not be used. In this case, it is more appropriate with a spring hanger which allows larger movements while still supporting the pipe. There are two types of spring hangers, variable-spring and constant-spring, with the obvious difference that the first applies a variable force on the pipe (depending on the spring deflection) and the second applies a constant force.

2. Rigid restraints
   Are usually cheaper and easier to maintain than supports which allow movement. Generally, they are used in positions where the pipe should be restrained or where the movement is expected to be low.

   - Struts
     Pre-engineered supports that is similar to the rod hangers but not restricted to vertical mounting.

   - Structural steel supports
     In some cases the best way to restrain a pipe is to build support out of structural steel. Vertical and lateral restraints can be achieved if the pipe is boxed in between four beams. Different kinds of attachment can be mounted between the pipe and the support to minimize the local pipe stress. A downside is that it requires more engineering time for the design.

   - Anchors
     When all degrees of freedom are restrained, the support is called an anchor. A typical anchor is constructed out of structural steel that the pipe can be directly welded to.

3. Snubbers
   Are dampers which permits slow movement (for example, thermal movement) but resists rapid acceleration (for example, due to fluid hammers or earthquake). It does not support any weight but can be paired together with a spring hanger that supports weight and permit thermal movement.

4. Sway braces
   Sway braces are not meant as supports but to limit the effects of pipe vibration. They use preloaded springs which counteracts the horizontal movement of the pipe. This raises the natural frequencies of the system.

In reality, the stiffnesses of pipe supports are not always linear. For example, the structural steel supports often include a small gap to allow for thermal expansion. This means that if, for example, a fluid hammer hits the pipe, the support stiffness in the gap direction will first be zero and then change instantaneously when the gap is closed. Another example of nonlinear stiffness is when a spring hanger reaches its maximum compression. In that case, the stiffness goes from the spring constant to, in most cases, a much higher value.

A very common tool to verify the structural integrity of pipes in Swedish nuclear power plants is Pipestress. This program is very useful as it verifies the pipe system directly according to ASME code [6]. Pipestress has some limitations, especially when it comes to support and boundary value modeling in dynamic analyses: A support can only be modeled with the same stiffness in every degree of freedom. This means that a sliding support, that in reality allows the pipe to move free in the upwards direction, will be modeled with the same stiffness both upwards and downwards. Neither can a support be modeled with a nonlinear stiffness. A gap or any other kind of nonlinearity will therefor be disregarded. A common way to include gaps larger than 5mm in the model is to first run an analysis

without any support in the gap direction. If the gap is exceeded, a constant stiffness is set and the analysis is remade. If not, the first analysis is used. A gap smaller than 5mm is usually ignored.

1.2 Purpose

As previously mentioned, gaps of different sizes between pipes and there supports occur frequently in the industry. That is the approximation to neglect gaps smaller than 5mm is also often used. The purpose of this thesis is to investigate if it is an accurate approximation or not. The approximation for larger gaps is also investigated.

A third objective is to determine the influence of support stiffness when there is an existing gap and if it is possible to refine the previously mentioned approximation via change of the support stiffness.

1.3 Limitations

The investigation will be focused on the simplified version of a main steam pipe system in a nuclear power plant. An actual main steam pipe will also be analyzed for comparison. The simplified system consists of a pipe with four bends and two rigid supports. A simple pipe break load will be used in the analysis. Gravity and loads due to insulation or fluid weight will not be considered. All supports will be modeled in the same way and the gaps will be of identical size. They will also only consist of one element each, connected to one node in the pipe model. Simple pipe elements, based on beam theory, will be used.

1.4 Approach

Both piping systems will be modeled and analyzed in the finite element software ANSYS [1], with and without supports containing gaps. Both systems will also be modeled without supports containing gaps in Pipestress. This is to verify the ANSYS model.

The analysis performed in ANSYS will be implicit finite element analysis, where the pipe system endures a pipe break time history load case. Both systems will be analyzed with a set of different gap sizes combined with standard support stiffnesses. The simplified system will be further investigated with respect to the influence of support stiffness combined with gap.

A model of the simplified system containing friction in the contact area between the pipe and its support will be investigated.

The final step is to compare the results and to draw conclusions regarding the accuracy of the support stiffness approximations.

2 Theory

To be able to perform dynamic structural as well as numerical analysis on pipe systems with both linear and non linear supports, a certain theoretical background is needed. In this chapter the required theoretical topics are briefly described. Starting with a concise summary of the Finite Element method, followed by a description of the Newton Rhapson iteration method, the Newmark beta time integration method, gap modeling, damping models and, finally, load cases.

2.1 Finite Element method

The finite element method is a numerical technique used to obtain approximate solutions to general partial differential equations [9]. To be able to solve complex structural problems in the aircraft industry the development of the finite element method began in the mid 1950s [15].

The characteristic manner of the finite element method is to divide the region, in which the differential equations are assumed to hold over, into smaller sub regions, finite elements. Hence approximate solutions are instead sought over each element rather that over the entire region. All finite elements together forms a finite element mesh [12].

Typical for the finite element method is that the governing equations which describes a physical problem are reformulated on weak integral form, through, for example, the principle of virtual work. Into the weak form the finite element approximations are introduced. This yields a spatially discretized set of ordinary differential equations that can be solved [8].

Different kinds of nonlinearities can occur when studying structural mechanics, for example material and geometrical nonlinearities. Hence this yields a nonlinear weak integral from that usually needs to be solved using an iterative technique, for example, the Newton Rhapson method [8].

2.2 Newton Rhapson

To be able to solve a nonlinear system of ordinary differential equations, for example, the discretized finite element equations, there are several different iterative solution methods available. In this section the Newton Rhapson method will be considered. The presentation of the Newton Rhapson method follows [17]. Let

$$\mathbf{g}(\mathbf{x}) = \mathbf{0} \tag{2.1}$$

where $\mathbf{x}$ denotes a displacement vector. The derivate of $\mathbf{g}$ is used as the Jacobian matrix,

$$\mathbf{J}(\mathbf{x}) = \frac{d\mathbf{g}(\mathbf{x})}{d\mathbf{x}}, \tag{2.2}$$

in the Newton Rhapson method. Linearizing of Eq. 2.1 around a guessed solution $\mathbf{x}^{(k)}$ yields the Taylor series expansion

$$\mathbf{g}(\mathbf{x}^k + \Delta\mathbf{x}^k) = \mathbf{g}(\mathbf{x}^k) + \mathbf{J}(x^k)\Delta\mathbf{x}^k + O((\Delta\mathbf{x}^k)^2) \approx \mathbf{g}(\mathbf{x}^k) + \mathbf{J}(\mathbf{x}^k)\Delta\mathbf{x}. \tag{2.3}$$
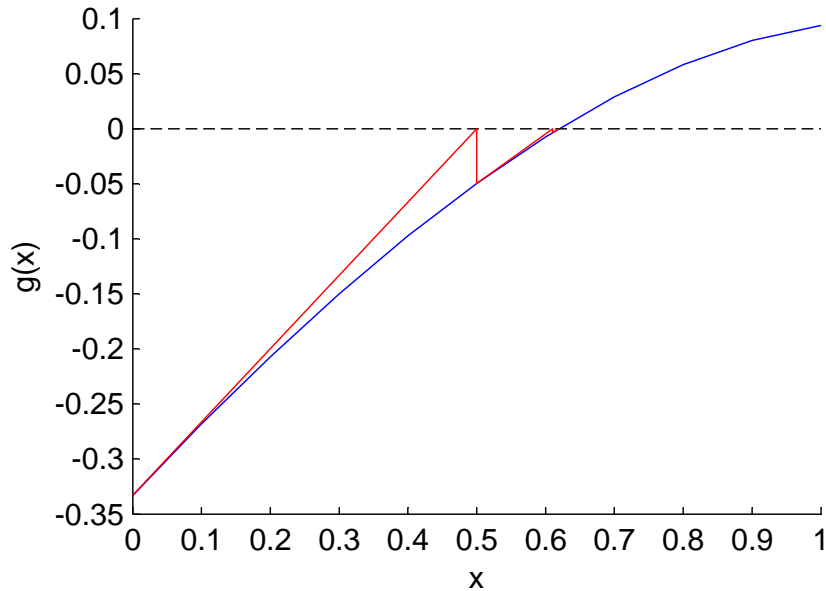
Figure 2.1: Example of Newton Rhapson iterations. Problem is $g(x) = x - \dfrac{1}{3}e^x = 0$. Three iterations are performed.

The Newton Rhapson method has quadratic convergence, hence rate of convergence is equal to 2. Figure 2.1 shows an example of Newton Rhapson iterations.

Using Eq. 2.3 a Newton Rhapson scheme can be formulated:

- Initial values $\mathbf{x}^{(0)} = \mathbf{x}^{(k)}$.

- Iteration Loop $i = 0, 1, ...$ until solution converges

  1. Compute $\mathbf{g}(\mathbf{x}^{(i)})$ and $\mathbf{J}(\mathbf{x}^{(i)})$.

  2. Compute $\mathbf{J}(\mathbf{x}^{(i)}) \Delta \mathbf{x}^{(i+1)} = -\mathbf{g}(\mathbf{x}^{(i)})$.

  3. Compute updated displacement $\mathbf{x}^{(i+1)} = \mathbf{x}^{(i)} + \Delta \mathbf{x}^{(i+1)}$

  4. Check convergence criteria

  $$||\mathbf{g}(\mathbf{x}^{(k+1)})|| \quad \begin{cases} \leq \text{TOL} & \rightarrow \quad \text{set} : \mathbf{x}^{(k+1)} = \mathbf{x}^{(i+1)}, \ \ \text{STOP} \\ > \text{TOL} & \rightarrow \quad \text{set} : i = i + 1, \ \ \text{go to 1} \end{cases}$$

2.3 Time integration

To obtain the solution of a initial value problems such as; an earthquake analysis on a piping system or a car crash simulation, a numerical method is needed to solve the time dependent response, there are two main kinds of schemes:

- **Explicit**, an explicit scheme uses exclusively values from previous time increments when solving for a solution at the updated time step $t_{(n+1)}$. Stabilization criterion limits the time step, hence small time steps are normally required.

- **Implicit**, an implicit scheme uses values from previous time increments, and from updated time steps $t_{(n+1)}$. This introduces a non linear equation system that needs

to be solved at each time step, for example, by using a Newton Rhapson method, see Section 2.2. Implicit schemes are unconditionally stable.

Both methods are frequently used to solve time dependent problems, the nature of the studied problem determines which method that are best suited.

2.3.1 Newmark method

A widely used scheme is the Newmark method. The presentation of the scheme follows the contents in [17]. Approximations on updated displacement, u_{n+1}, and velocity, v_{n+1}, at time t_{n+1} are the base of the method,

$$
\begin{aligned}
u_{n+1} &= u_n + \Delta t v_n + \frac{(\Delta t)^2}{2}[(1 - 2\beta)a_n + 2\beta a_{n+1}] \\
v_{n+1} &= v_n + \Delta t[(1 - \lambda)a_n + \lambda a_{n+1}]
\end{aligned}
\tag{2.4}
$$

where β and λ are parameters that controls the convergence, stability and accuracy of the solution. Depending on how those parameters are chosen the Newmark method can be either explicit and implicit. As previously mentioned, an implicit scheme uses both known quantities from previous times and quantities from updated times t_{n+1}, by choosing $\beta = 1/4$ and $\lambda = 1/2$ the scheme is implicit.

According to a mathematical analysis, [7], of the Newmark method, limiting inequalities on β and λ were established as

$$
0 \le \beta \le 0.5
$$
$$
0 \le \lambda \le 1.
$$

By using approximate values on u_{n+1} and v_{n+1} and introducing those into the spatial discretized form of the equations of motion and solving with, for example, the Newton Rhapson method, the unknown accelerations a_{n+1} can be determined. Then Eq. 2.4 and a_{n+1} yield the unknown displacements and velocities at time t_{n+1}.

2.4 Gap Modeling

A boundary value problem that involves contact occurs frequently in almost all scientific disciplines. Due to the characteristics of a contact problem it is highly nonlinear and hence demands large computer resources. Historically contact mechanics problems were often approximated by special assumptions, or special design codes that compensates for contacts for each case, for example, in ASME [5], but the improvements within the computer technology allow todays engineers to numerically solve contact problems using both implicit and explicit finite element analyses.

Contact boundary value problems can be divided into two general groups, rigid-to-flexible and flexible-to-flexible. A general formulation of a one dimensional case of rigid to flexible contact is presented below and follows [16].

2.4.1 General formulation

Consider the static frictionless contact problem consisting of a point mass m and a spring with stiffness k that supports a mass. The point mass experiences a gravitational load and

its displacement u is restricted via a rigid support, see Figure 2.2. The potential energy of the system can be expressed as
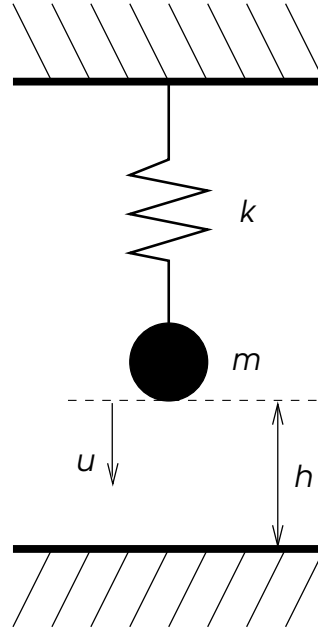

Figure 2.2: Schematic overview of spring-point mass system.

$$\Pi = \frac{1}{2}ku^2 - mgu. \tag{2.5}$$

If the displacement restriction is not considered, the extremum of Eq.2.5 is computed via variational calculus, the first variation becomes

$$\delta\Pi(u) = ku\delta u - mg\delta u = 0. \tag{2.6}$$

While the second variation of Π becomes

$$\delta^2\Pi = k \tag{2.7}$$

Equation 2.7 yields that the extremum of Eq. 2.5 is a minimum, at which the displacement $u = \frac{mg}{k}$. In Figure 2.3 the potential energy of the system is shown. When the displacement restriction is considered, the restricted motion of the mass can be described by

$$c(u) = h - u \geq 0 \tag{2.8}$$

where h is the distance between the mass and the support. While $c(u) \geq 0$ there is a gap between the mass and the rigid support, $c(u) = 0$ states that the gap is closed.

Variation of Eq. 2.8 yields $\delta u \leq 0$, hence the rigid support restricts the variation δu. Thus must the virtual displacement fulfill the constraint. The use of the restricted variation in Eq. 2.6 yields an variational inequality

$$ku\delta u - mg\delta u \geq 0, \tag{2.9}$$

when the gap is closed the gravitational force mg is larger than the spring force ku thus the greater sign in the variational inequality. The solution to Eq. 2.5 is not at the point corresponding to Π_{min}, it is at the point associated to $\Pi_{\mathrm{min}}^{\mathrm{c}}$ because of the decreased solution space caused by the motion constraint, see Figure 2.3. The solution associated to Π_{min} is where the system has minimal energy within the restricted solution space.
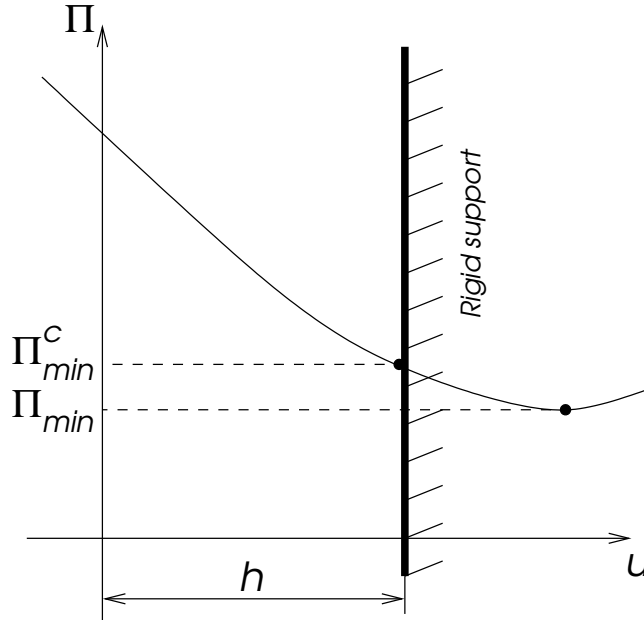
Figure 2.3: Plot of the spring-point mass system potential energy, both with and without rigid support.

At the contact point both a test function, v, and the solution, u, have to fulfill $v - h \leq 0$. Equation 2.6 can be expressed using the difference between the test function and the solution, $\delta u = v - u$,

$$ku(v - u) - mg(v - u) = 0 \tag{2.10}$$

instead of using the variation. At the contact point the gravitational force is larger than the spring force, $mg > ku$, and the fact that $v - h = 0$, this yield

$$ku(v - h) \geq mg(v - h). \tag{2.11}$$

The variational inequalities in both Eq. 2.9 and Eq. 2.11 that characterize the solution of u are directly linked to the inequality in Eq. 2.8. To be able to solve the contact problem the variational inequalities cannot be directly used, special methods are required, two method that are widely used are described in the Section 2.4.4 and 2.4.5.

2.4.2 Reaction force

In the manner of classical contact theory regarding non-adhesive contact no tension force is allowed in the contact area. In the previous example with the point mass, a reaction force appears directly when the mass is in contact with the support. The assumption regarding non-adhesive contact on the previous example yields a restriction in the reaction force

$$R_N \leq 0 \tag{2.12}$$

and two possibilities remain:

- The gap is open, the spring force ku exceeds the gravitational force mg.

$$c(u) > 0$$
$$R_N = 0 \tag{2.13}$$

- The gap is closed, the point mass is in contact with the rigid support.

$$c(u) = 0$$
$$R_N < 0 \tag{2.14}$$

If the two cases are combined they can form the statement

$$c(u) \geq 0$$
$$R_N \leq 0 \tag{2.15}$$
$$R_N c(u) = 0$$

known as a Hertz-Signorini-Moreau condition. In Figure 2.4 the gap size, Equation 2.8, is plotted versus the reaction force. One point of the curve is not differentiable, thus non-smooth mathematical methods are to be applied.
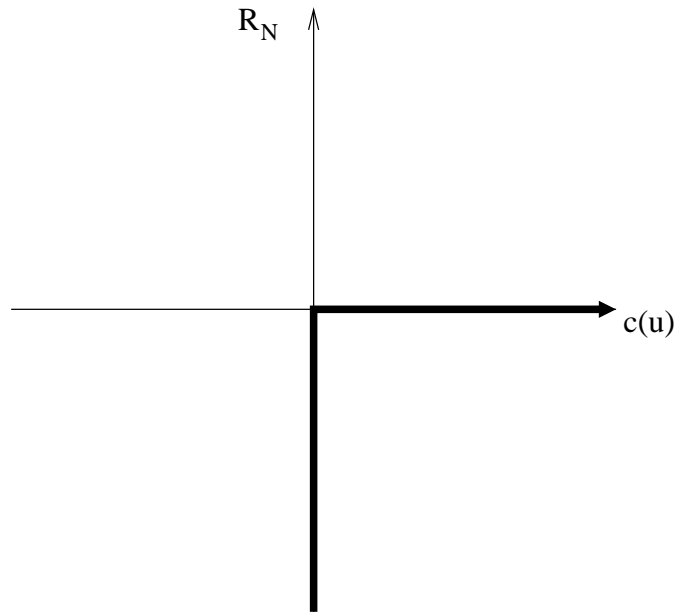

Figure 2.4: Plot of reaction force versus $c(u) = h - u$.

2.4.3 Friction

If the gap is assumed to be closed, the point mass is in contact with the rigid support thus $R_N < 0$. In the case of friction, a external force, F_T, is added in the tangential direction to the rigid supports plane. Free body diagram is shown in Figure 2.5 and equilibrium equations for the system. A simple friction model, Coulomb's law, is adopted to describe friction in the contact between the point mass and the support. Two states exist: stick and slip. Stick allows no motion between the mass and the support, while a certain relative motion between the support and the mass, u_T, is allowed when slip occurs. This yields three different cases:

1. Coulomb's law yields an inequality

$$f(R_N, R_T) = |R_T| + \mu R_N \leq 0. \tag{2.16}$$

Where μ is the friction coefficient. This relationship can now be used to separate between stick and slip.
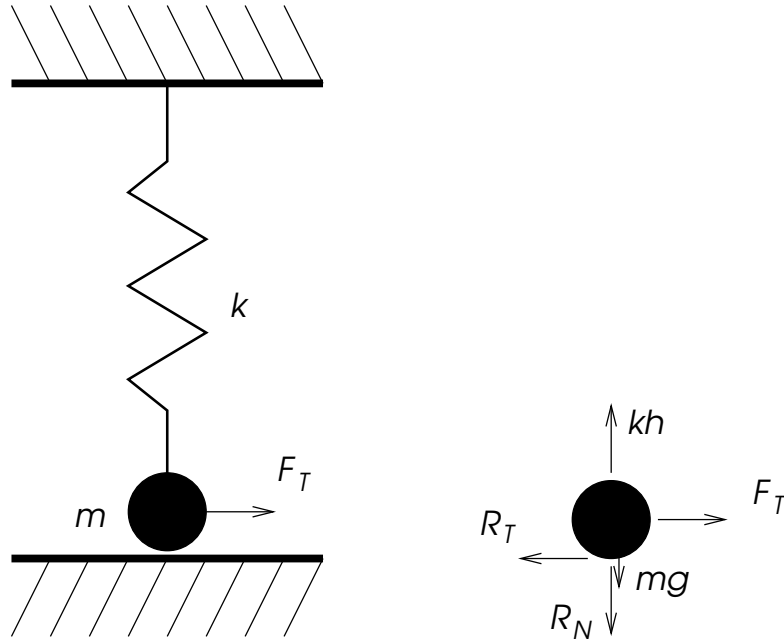
Figure 2.5: Free body diagram of spring-point mass system.

2. When stick occurs

$$|R_\mathrm{T}| < -\mu R_\mathrm{N}, \tag{2.17}$$

hence no motion between the mass and the support, $u_\mathrm{T} = 0$. Yields the reaction force R_T.

3. Finally slip occurs when

$$|R_\mathrm{T}| = -\mu R_\mathrm{N}, \tag{2.18}$$

hence relative motion between mass and spring, $u_T \neq 0$. R_T can be established from Eq. 2.18.

Also as for Eq. 2.15 these equations forms a Kuhn-Tucker condition.

$$\begin{aligned} |u_T| &\geq 0 \\ f &\leq 0 \\ f|u_T| &= 0 \end{aligned} \tag{2.19}$$

In Figure 2.6 a relationship between R_T and u_T is plotted. As for 2.4 non differentiable points in the plot of force versus deflection exist, which cause mathematical difficulties.
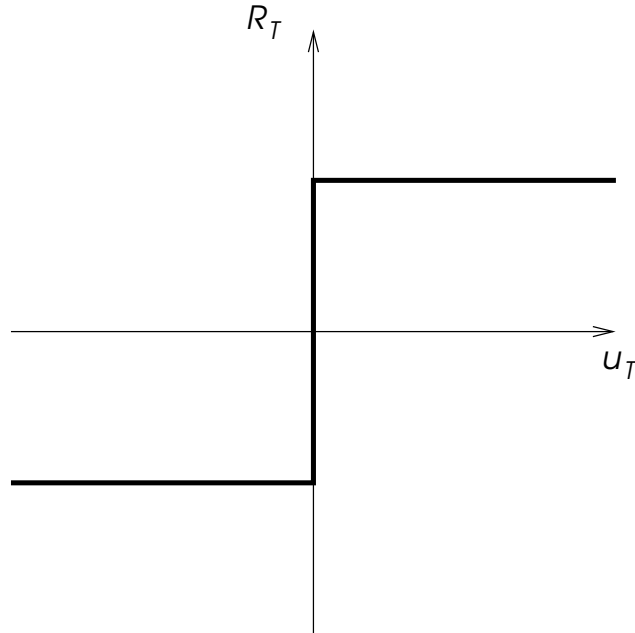
Figure 2.6: Tangential force against displacement.

2.4.4 Lagrange Multiplier Method

One method to obtain a solution to a contact problem that is constrained by an inequality Eq. 2.8, is the Lagrange Multiplier. According to [16], assume that the contact is active, hence the conditions in Eq. 2.14 is fulfilled. In that case the Lagrange Multiplier method contributes with a term to the systems potential energy, Eq. 2.5. The term contains the motion constraint.

$$\Pi(u, \lambda) = \frac{1}{2}ku^2 - mgu + \lambda c(u) \tag{2.20}$$

From Eqs. 2.20 and 2.15 one can conclude that the reaction force R are equivalent to λ. By variation of Equation 2.20, δu and $\delta \lambda$ can be varied independently, two equations are established, namely

$$ku\delta u - mg\delta u - \lambda\delta u = 0 \tag{2.21}$$

$$\delta\lambda c(u) = 0 \tag{2.22}$$

The equilibrium equation of the mass with the contribution from the reaction force when the mass is in contact with the rigid support are stated in Eq. 2.21, and the second equation of the two above represents the fulfillment of the motion constraint, Eq. 2.8, see Figure 2.7 . Hence the previous restriction on the variation no longer applies, and it is possible to solve for λ thus also for R_N

$$\lambda = kh - mg = R_N. \tag{2.23}$$
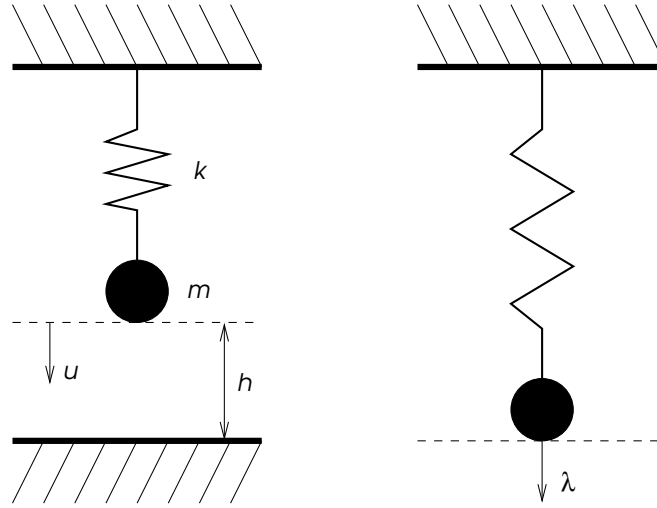
Figure 2.7: Schematic overview of spring-point mass system with Lagrange multiplier.

2.4.5   Penalty Method

Another method widely used to solve contact problems in finite element analysis is the Penalty method. When the constraint is active, the point mass is in contact with the rigid support and a penalty term is added to the energy in Eq. 2.5, which yields

$$\Pi = \frac{1}{2}ku^2 - mgu + \frac{1}{2}\epsilon[c(u)]^2 \quad \text{with } \epsilon > 0 \tag{2.24}$$

A comparison between the additional energy penalty term in Eq. 2.24 and the energy of a simple spring shows that their structure are equal, hence ϵ can be construed as a spring stiffness on a spring in the contact between the mass and the rigid support, see Figure 2.8. Variation of Equation 2.24 in the case of contact yields

$$ku\delta u - mg\delta u - \epsilon c(u)\delta u = 0 \tag{2.25}$$

and the solution u then becomes

$$u = \frac{(mg + \epsilon h)}{k + \epsilon} \tag{2.26}$$

and the corresponding motion constraint equation reads

$$c(u) = h - u = \frac{kh - mg}{k + \epsilon} \tag{2.27}$$

When contact occurs $mg \geq kh$, and according to the constraint Equation 2.27 the mass will penetrate into the rigid support. This is physically equal to compression of the spring in the contact, see Figure 2.8. Two limiting cases can be determined in the Penalty method, since the gap Eq. 2.27 is only fulfilled in the limit $\epsilon \to \infty \Rightarrow c(u) \to 0$:

1. $\epsilon \to \infty \Rightarrow u - h \to 0$, hence for large values on ϵ the spring stiffness is large, hence small penetration occurs and the right solution, u, is approaching.

2. $\epsilon \to 0$ is valid when there is no contact, hence inactive constraints. If contact occurs when ϵ is small a solution with large penetration would occur.

Using Eq. 2.25 the reaction force is obtained,

$$R_N = \epsilon c(u) = \{\text{in this case}\} = \frac{\epsilon}{k + \epsilon}(kh - mg). \tag{2.28}$$

When $\epsilon \to 0$ Eq. 2.28 yields the same solution as with the Lagrange multiplier method Eq. 2.23.
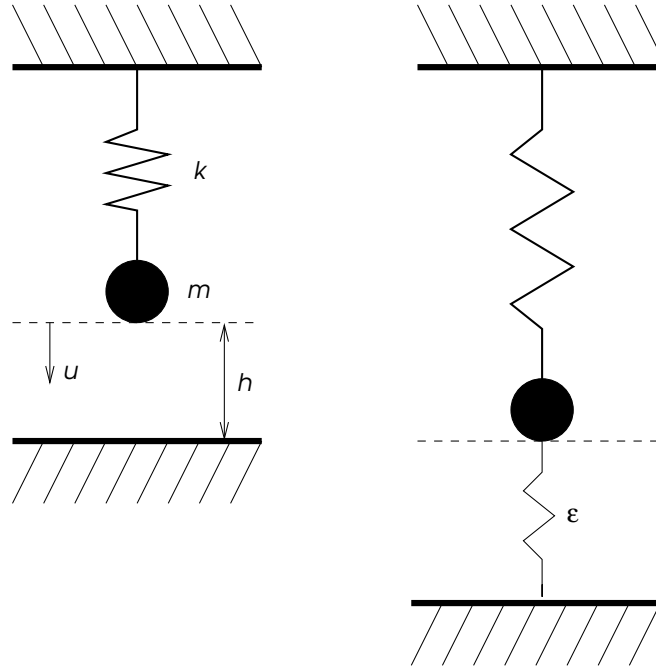
Figure 2.8: Spring-point mass system, with and without additional penalty spring.

2.5 Damping

For all structural dynamic analyses, an equation of motion is formulated. The linear spatially discretized equation of motion under externally applied time dependent forces can be written as

$$\mathbf{M}\ddot{\mathbf{u}}(t) + \mathbf{C}\dot{\mathbf{u}}(t) + \mathbf{K}\mathbf{u}(t) = \mathbf{F}(t) \tag{2.29}$$

where $\mathbf{M}$ is the mass matrix, $\mathbf{C}$ is the damping matrix, $\mathbf{K}$ is the stiffness matrix and $\mathbf{F}(t)$ is the external load vector. In this section two examples of damping will be discussed, more specifically; Rayleigh damping and constant damping.

The modeling of damping of large systems is usually quite complicated. The knowledge about how to model damping for a multiple degree of freedom system is limited and often the most effective way is to describe it as Rayleigh damping. It is assumed that the damping matrix is proportional to a combination of the mass and stiffness matrices in the following manner

$$\mathbf{C} = \alpha\mathbf{M} + \beta\mathbf{K} \tag{2.30}$$

where α and β are predefined constants. An orthogonal transform using the undamped modes of this damping matrix leads to the following expression

$$2\zeta\omega_i = \alpha + \beta\omega_i^2 \tag{2.31}$$

where ω_i is the eigenfrequency and ζ is the damping ratio. The latter can be rewritten as

$$\zeta = \frac{\alpha}{2\omega_i} + \frac{\beta\omega_i}{2} \tag{2.32}$$

$\zeta=1$ means critical damping. Unlike constant damping, Rayleigh damping varies with frequency. The α and β constants are usually determined so that the damping curve match two damping values. These values do often belong to the lowest and highest eigen frequencies of interest, or measured values. For example shown in Figure 2.9 is a constant damping of 5% as well as the two different parts of 2.32. Its clear that the α-part (mass
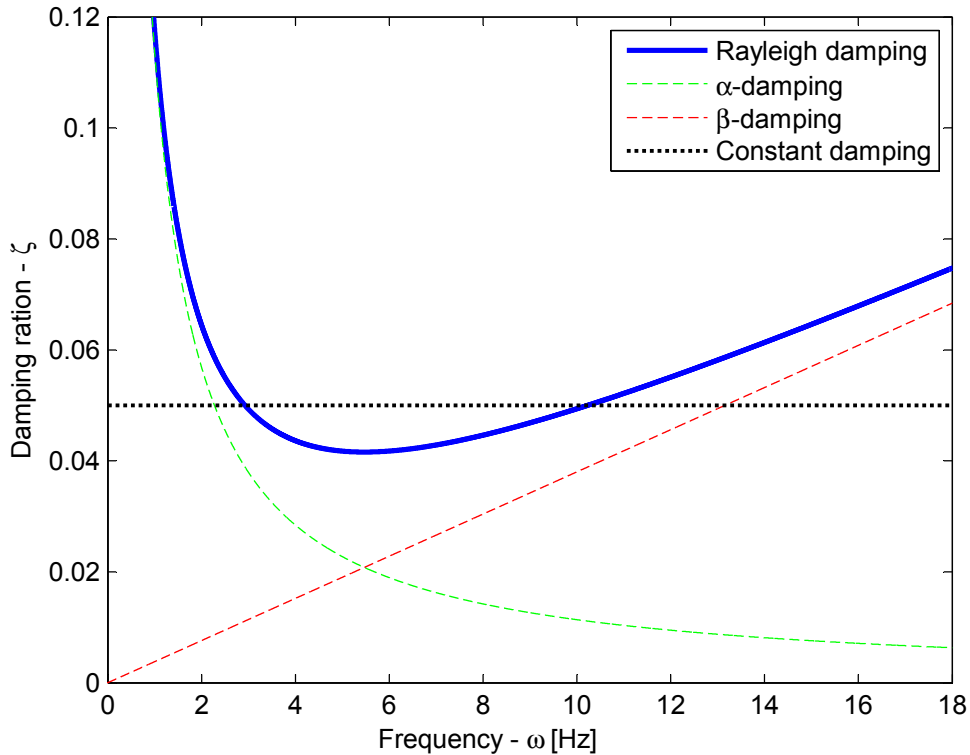
Figure 2.9: Rayleigh damping and constant damping curves

matrix part) determines the low frequency damping and that the β-part (stiffness matrix part) determines the high frequency damping.The values of α and β in this example are α=0.2275 Hz and β=0.0076 1/Hz.

2.6 Load cases

Loads that are applied to a piping system in small time portions relative its total life time are often called occasional loads. Examples of occasional loads are extreme weather loads such as tornadoes, hurricanes and earthquakes. Other examples are postulated nuclear power plant accidents such as pipe breaks and loss of coolant. Only pipe break loads will be considered in this section.

2.6.1 Loads caused by Pipe break

A pipe break in a high energy system may cause serious consequences. The abrupt change in flow characteristics from a full separation pipe break creates a pressure difference that travels along the pipe. According to [11] a conservative approach is to approximate the resulting jet force F_j induced by the pressure difference by:

$$F_j = A_e(C_t P_0 - P_a) \equiv C_t P_0 A_e \tag{2.33}$$

where A_e is equal to exit area at break, P_0 is equal to initial pressure at source, P_a is equal to ambient pressure and C_T is equal to the thrust coefficient. In [10] a less conservative approach to approximate the jet force is presented.

Figure 2.10 shows a schematic overview of the steam piping system that has been subjected to a pipe break, while Figure 2.11 shows the resulting force components versus time.
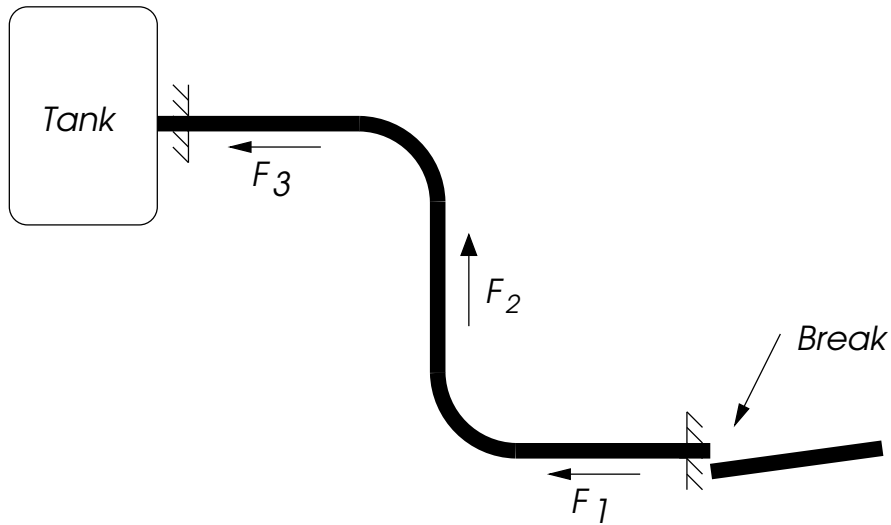
Figure 2.10: Schematic view of pipe system after pipe break.
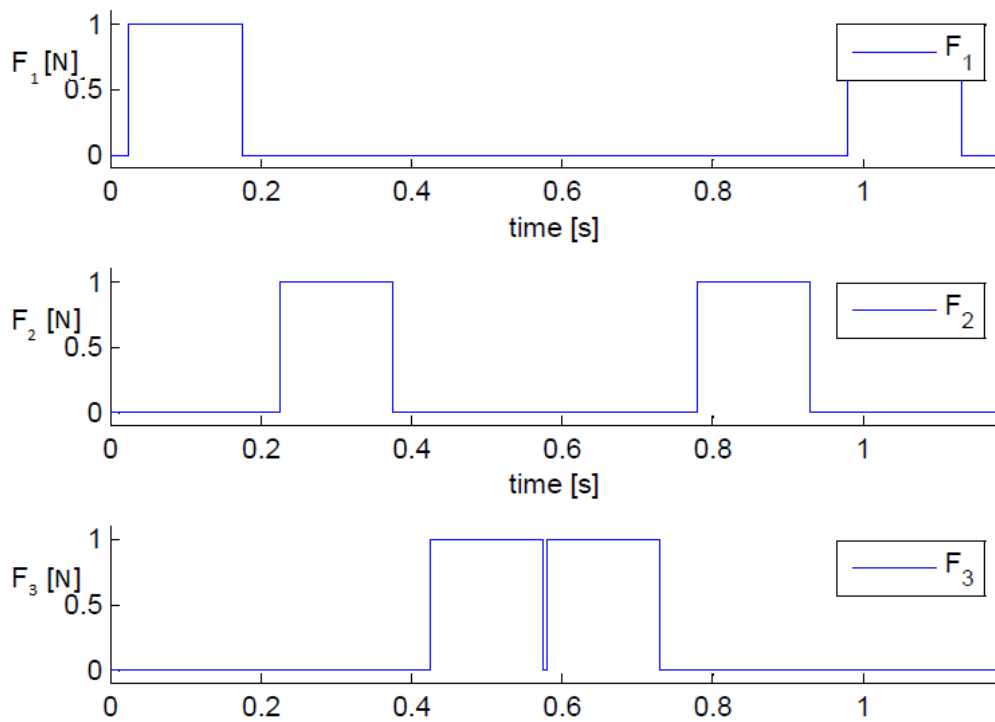
Figure 2.11: Force components from schematic pipe subjected to a pipe break. Break occurs at time=0.

3 Method

The approach for this thesis was to study both a *typical piping system*, TPS, (from a typical power plant) and a *simplified piping system*, SPS. In Section 3.1 and 3.2 the systems are described thoroughly. ANSYS was mainly used for the piping analysis. As mentioned in section 1.1 Pipestress is commonly used in the Swedish nuclear industry. Due to this, the ANSYS finite element model was verified against a Pipestress finite element model.

3.1 Simplified piping system

This system is constructed to resemble a steam system that is ranging between a pressure control tank and the main steam system, see Figure 3.1. The pipe system is subjected to a pipe break load, see Section 2.6.
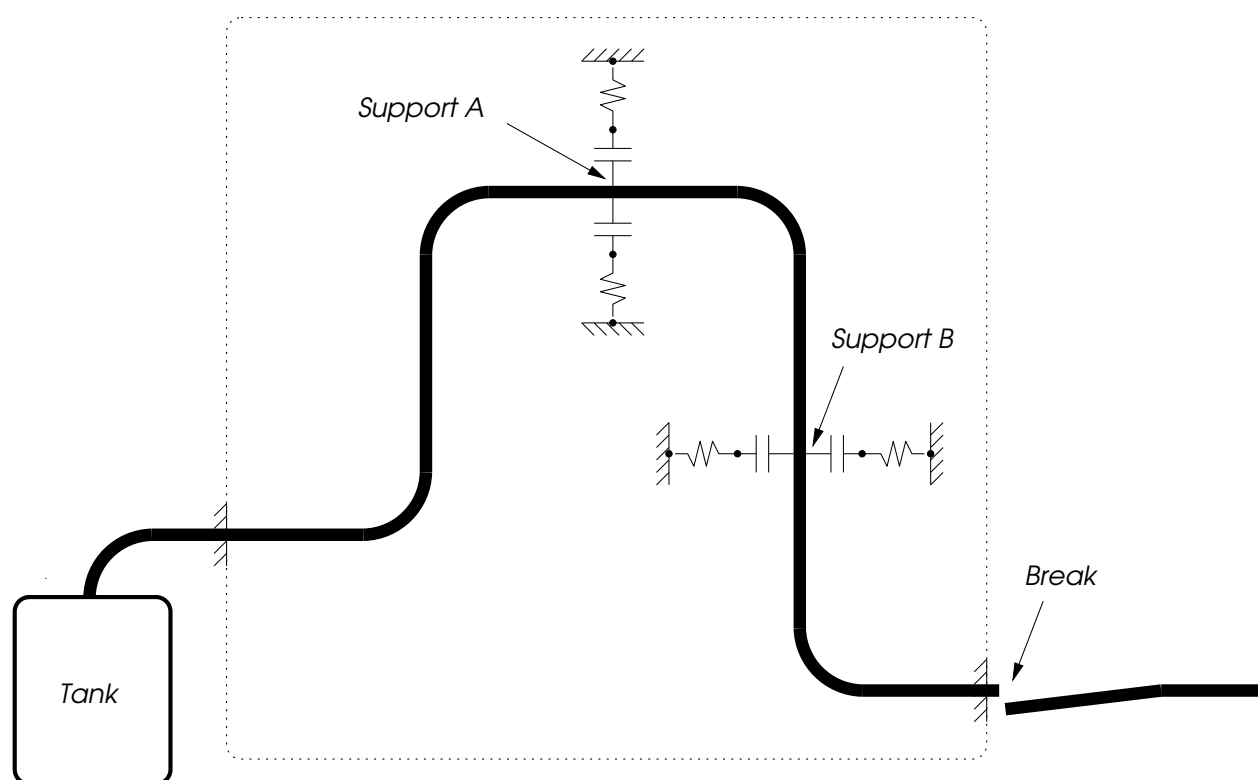
Figure 3.1: Simplified piping systems, geom1.

3.1.1 Geometry and Material data for the simplified system

One base geometry was created, *geom1*, see Figure 3.1. Geom1 consists of three bends, two supports (one vertical and one horizontal) and two anchor points. One of the geometry parameters was then alternated in four steps in the base geometry which created four versions of geom1, see Table 3.1.1 and Figure 3.2 for dimensions and cross sectional data. All supports except the anchor points are structural steel supports, with a gap,c, between the pipe and the support see Figure 3.4. The material used for the pipe in the analysis was *SA155 Gr C55*, see Table 3.1.1 for material properties, which is a typical steel used for high pressure service, see [6] for further information regarding material.
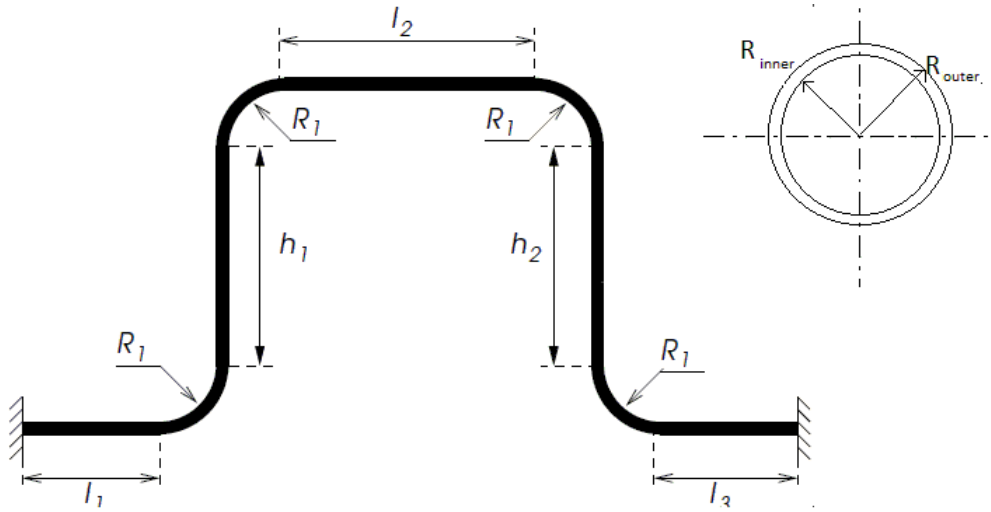
Figure 3.2: Simplified piping systems, geom1.

Table 3.1: Geometrical data and material data for geom1

	h_1 [m]	h_2 [m]	l_1 [m]	l_2 [m]	l_3 [m]	R_1 [m]
geom1_v_1	13	13	16.5	16.5	16.5	1
geom1_v_2	15	13	16.5	16.5	16.5	1
geom1_v_3	17	13	16.5	16.5	16.5	1
geom1_v_4	19	13	16.5	16.5	16.5	1

	R_{inner} [m]	R_{outer} [m]
geom1	0.365	0.381

	E [Pa]	ν [ ]	ρ $[\frac{\text{kg}}{\text{m}^3}]$
geom1	195e9	0.3	7850

3.1.2 Finite element model for the simplified system

A finite element model of the piping system was modeled in ANSYS with the linear elastic elements pipe16 and pipe18, Figure 3.3 displays the calculation domain. See [2] for more information regarding the elements used to model the pipe. The supports were modeled in two manners, one with combin14 spring elements and the other one was modeled with conta178 contact element and combin14 spring elements connected in series, see Figure 3.4. The lagrange multiplier method was used in the contact surface normal-direction and the Penalty method was used in contact surface tangential-(frictional) direction, see Section 2.4.
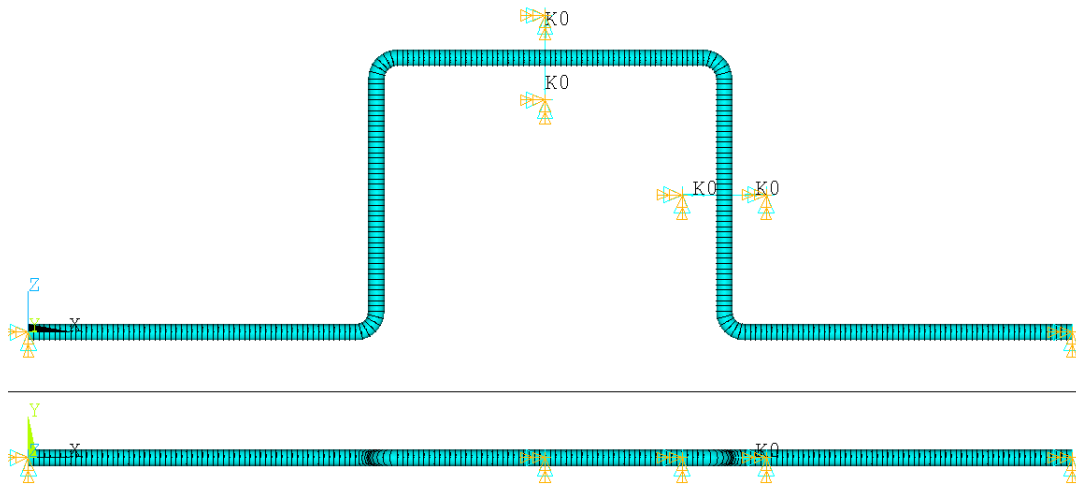
Figure 3.3: Calculation domain for geom1.v1.
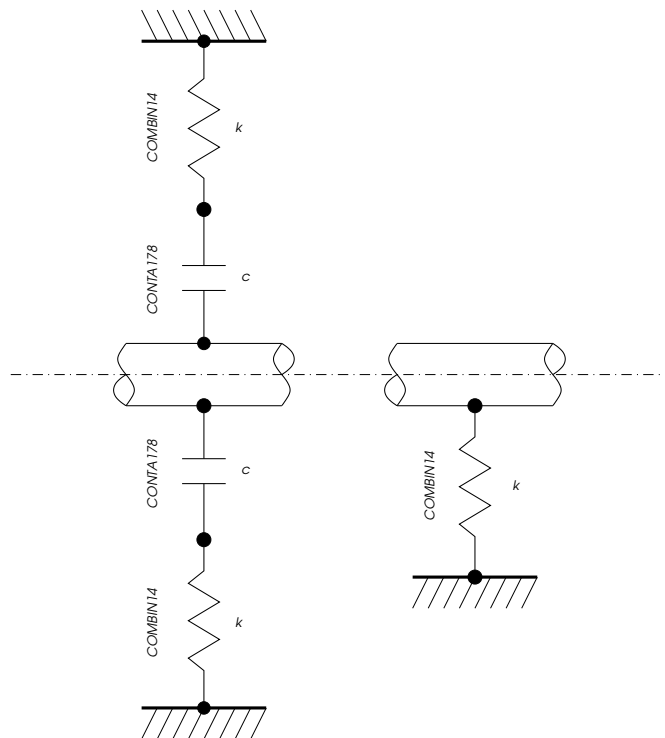
Figure 3.4: Schematic figure over a support modeled with conta178 and combin14 elements to the left and a support modeled with combin14 to the right.

3.1.3 Analysis of the simplified system

Here we present the settings that are similar in all of the various analyses that were conducted for the SPS. All analyses hereinafter defined for the SPS are implicit finite element analyses with time history loading that are performed in ANSYS.

Load

The load case acting on the SPS was a pipe break, where the break occurred directly downstream the second anchor point, see Figure 3.1. Before the break, the steam pressure was 70 bar and the steam temperature was 559 Kelvin. The pipe break results in axial forces F_1–F_5 acting on the pipe, see Figure 3.5. See Appendix A for plots over force components 1-5, and Section 2.6 for further information regarding the load scenario.
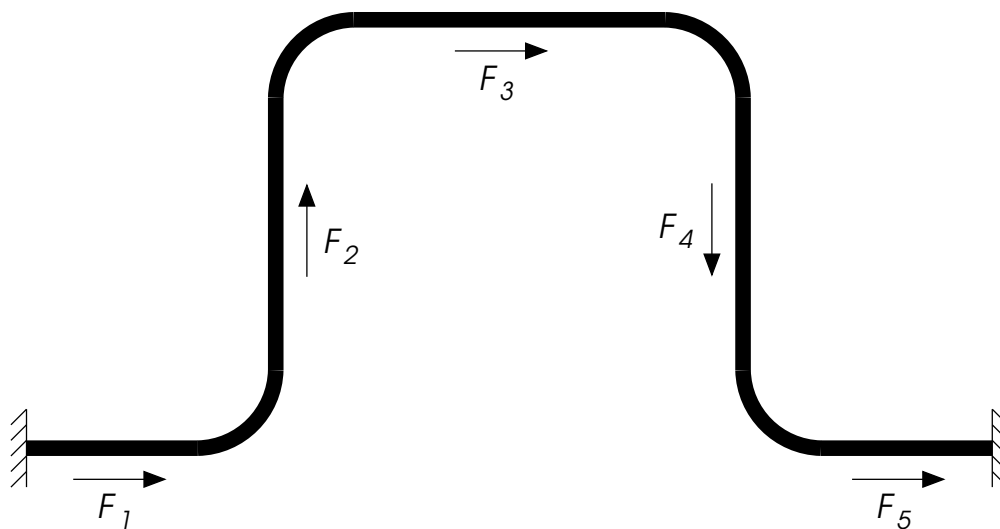
Figure 3.5: Forces acting on SPS due to pipe break.

Damping

Rayleigh damping was adopted. The Rayleigh damping parameters α and β were chosen to approximate 5% constant dampingin in the range between the lowest and highest considered eigen frequency. This is the current standard according to the ASME norm [5]. The Rayleigh damping, used in all analyses, is shown in Figure 3.6. The dotted line in the figure represents the lowest eigenfrequency of the system.

Time stepping

A Newmark time integration scheme were adopted, see Section 2.3.1.

Assumptions

Gravity and the weight of pipe insulation were not considered. The mass of the fluid was neglected.

The analyses that were conducted for the simplified geometry in this thesis is presented in the following sections 3.1.3.1 - 3.1.3.4.
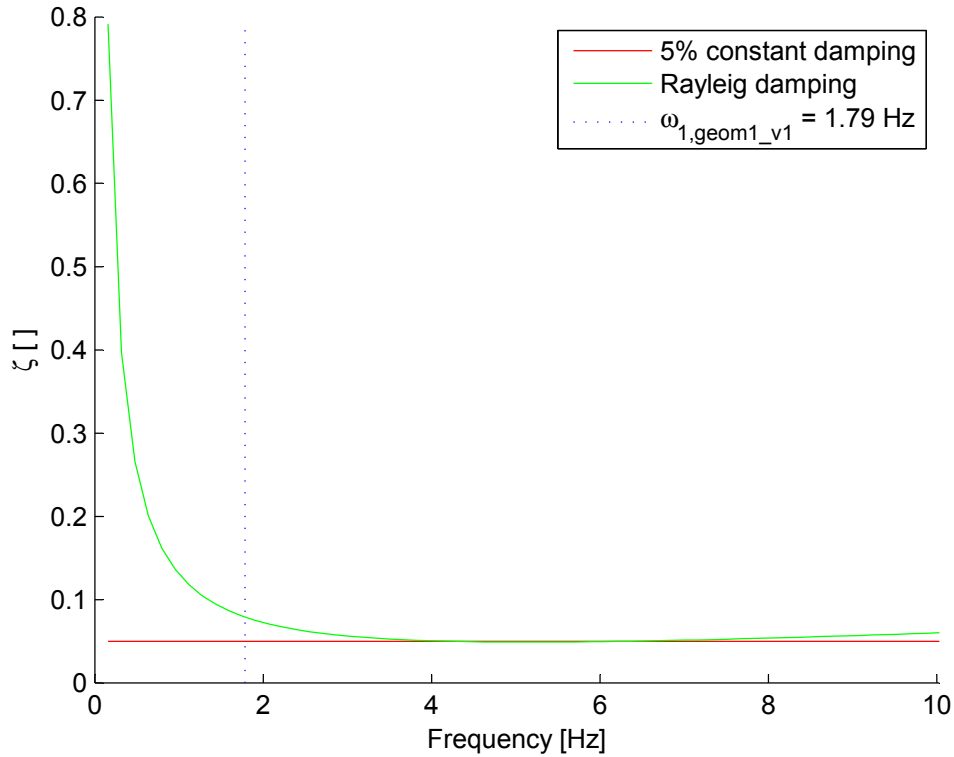
Figure 3.6: Rayleigh curve $\alpha = 1.5814$ Hz, $\beta = 0.0015093$ 1/Hz and $\omega_{1,geom1}$ is the lowest eigenfrequency of the system.

3.1.3.1 Time step evaluation

When the piping system is subjected to a time history pipe break load, the gaps between the supports and the pipe will occasionally be closed. Hence the pipe will experience high decelerations and due to this high amplitude short duration impact forces arise in the contact between the pipe and the supports.

To be able to resolve those short duration forces sufficiently small time steps were needed. In the time step evaluation analysis, the time steps were incrementally lowered according to

$$timestep(i) = 0.001 \left(\frac{2}{3}\right)^{(i-1)} \text{ [s]} \tag{3.1}$$

where i is the current increment. The time step size was lowered until both maximum contact force and maximum pipe stress converged.

The gap size used in the analysis corresponds to the case where highest stresses in the pipe occur and impact between the pipe and the supports takes place at least two times. Both support A and B had the equal initial gap size. Geom1 version one was used in the analysis.

3.1.3.2 Contact surface friction

The influence of friction in the contact was investigated on the simplified piping system. As mentioned in Section 3.1.2, when friction is considered the Penalty method is used in

the contact planes tangential directions with μ as the friction coefficient, combined with Lagrange multiplier method in the contact planes normal directions, see Section 2.4.5.

The gap sizes were chosen so that support A experienced maximum deformation in the contact normal direction. Three different gap sizes were analyzed each of them corresponding to an local maximum point in a "max support deformation versus gap size" plot. Both support A and B had equal initial gap size in the three simulations performed. Geom1 version one were used in the analysis.

3.1.3.3 Support stiffness

The occurrence of support reaction force impulses made it very interesting to examine the influence of the modeled support stiffness, both for a support with and without gaps. The purpose was to lower the stiffness and therefor also lower the deceleration of the pipe hitting the support. This should in theory eliminate the reaction force spikes. The first version of the simplified piping system was chosen, see Section 3.1.1, and the supports were modeled with a 25.7mm gap. Previous analyses of this system, with standard support stiffness of 700kN/mm, showed that this gap size gave rise to the highest pipe stresses. The system with and without a gap was then analyzed with twenty different support stiffnesses, with the largest one being the standard stiffness, according to the formula following

$$k(i) = 18.2588(1.2^i) \ [\text{kN/mm}] \tag{3.2}$$

$$i = 1 : 20$$

In Figure 3.7 the stiffness $k(i)$ versus increments, i is plotted. It was also interesting to investigate if one could approximate the behavior of a gap support by varying the stiffness of support without a gap. To see the effects of this clearly, the extreme values 700kN/mm and 21.9kN/mm were compared. Booth the reaction force of support A and the stress of the adjacent element were investigated.

3.1.3.4 Gap size

In this analysis the four different versions of geom1 were analyzed,$v_1 - v_4$, see Table 3.1.1. A gap, c, existed between the pipe and its supports and the influence of the size of this gap was studied. The gap size was incrementally changed in 43 steps for each of the four geometries, according to:

$$c(i) = 0.0001(i - 1)^{2.41} \ [\text{m}] \tag{3.3}$$

were i is the current increment numbers and changes according to

$$i = 1 : 43.$$

The curve that represents the initial gap size is displayed in Figure 3.8. The gaps were equally changed in both support A and B. Friction in the contact between the supports and the pipe was neglected.
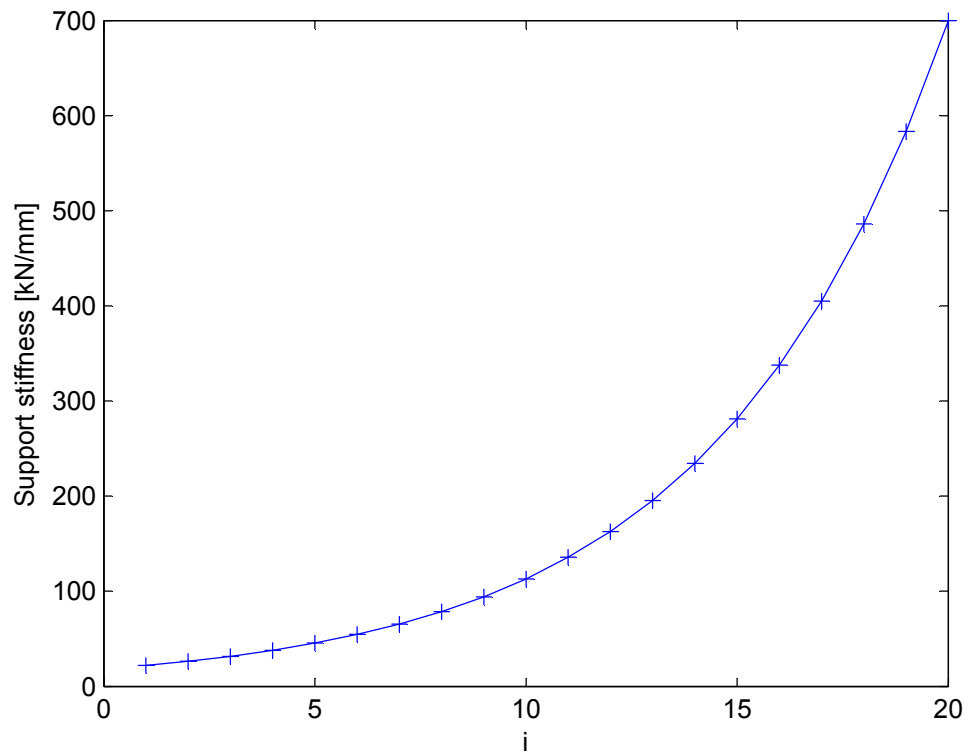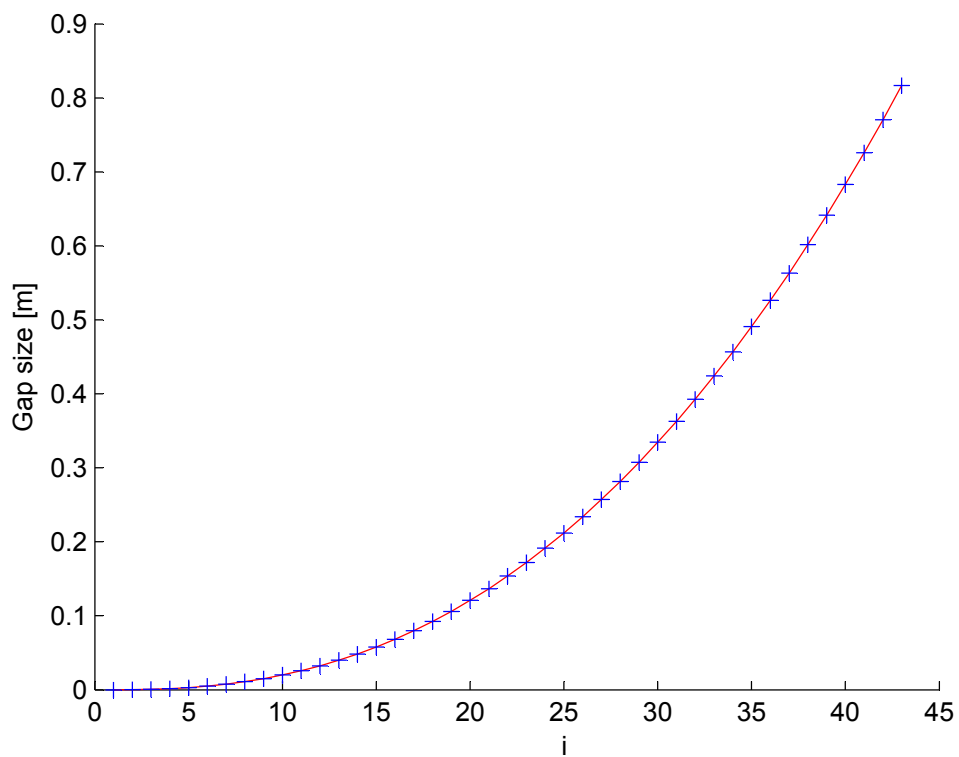
Figure 3.7: Stiffness versus increments.

Figure 3.8: Initial gap size versus increments.

3.2 Typical piping system

This system is a typical main steam system that is ranging form the steam generator until the containment wall. Then the system continuous through the containment wall towards the turbine. In this thesis the part of the system that is inside the containment was analyzed during a typical pipe break further downstream on the outside of the containment. The piping system belongs to ASME safety class 1 and the load scenario is level D.
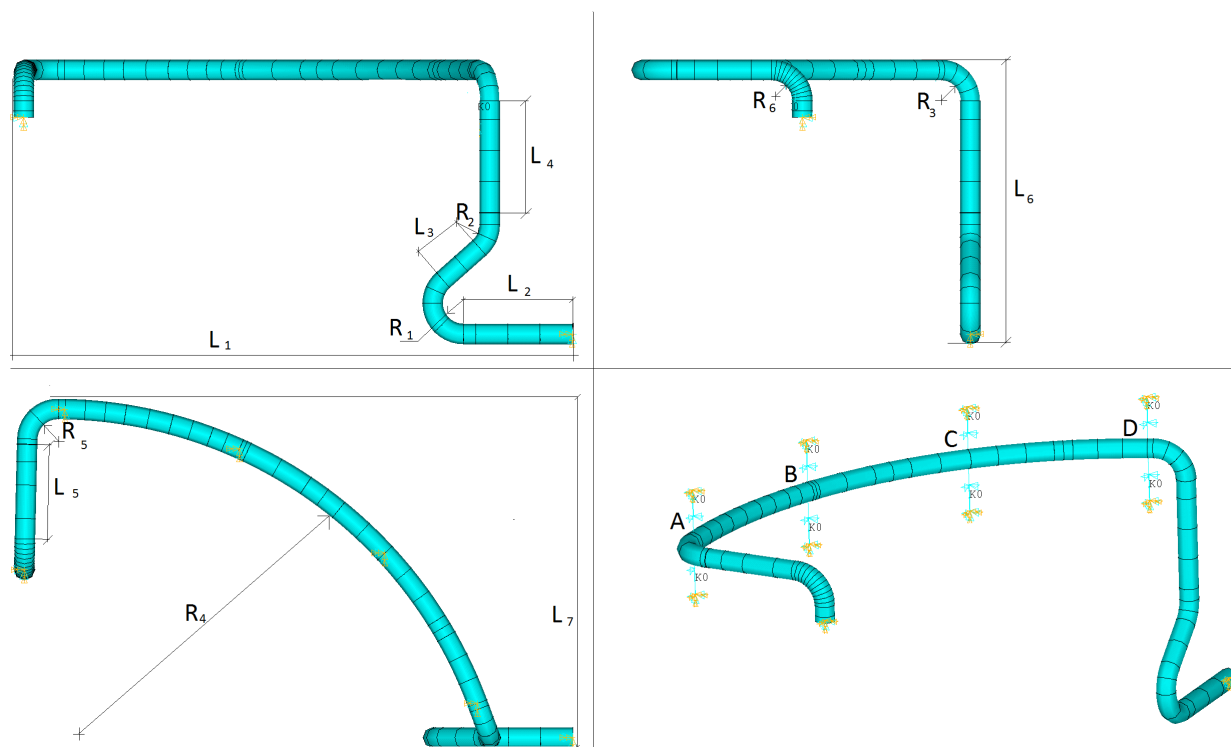
Figure 3.9: Typical piping system with anchors and supports.

3.2.1 Geometry and Material data for the typical piping system

The analyzed part of the TPS contains of two anchor points and four pipe supports see Figure 3.9. The first anchor point is situated where the pipe is connected to the steam generator and the second one is situated where the pipe reaches the containment wall. The supports are of rigid restraint type, see Section 1.1 hence a rigid frame built up by construction steel and there exists a gap between the pipe and the support. Material is *SA155 Gr C55* which is a typical steel used for high pressure service, see [6].

The dimensions of the piping system are displayed in Figure 3.9, cross section data and material data are stated in Table 3.2.1.

3.2.2 Finite element model of the typical piping system

A finite element model of the system was created in ANSYS. The pipe was modeled with linear elastic elements pipe16 and pipe18, see ANSYS manual, [2], for more information regarding the elements. Figure 3.10 displays the calculation domain. The rigid restraint supports were modeled with conta178 and combin14 elements see Figure 3.4. Conta178 is

Table 3.2: Geometrical data and material data for TPS

L_1 [m]	L_2 [m]	L_3 [m]	L_4 [m]	L_5 [m]	L_6 [m]	L_7 [m]
19.5	4	1.4142	5	4.5	10	12

R_1 [m]	R_2 [m]	R_3 [m]	R_4 [m]	R_5 [m]	R_6 [m]	
1.14	1.14	1.14	15	0.85	1.14	

R_{inner} [m]	R_{outer} [m]
0.365	0.381

E [Pa]	ν [ ]	$\rho \left[\frac{\text{kg}}{\text{m}^3}\right]$
195e9	0.3	7850

a node-to-node contact element, that can use both the Lagrange multiplier method and the Penalty method to model the gap. Lagrange multiplier method was used in this case and friction was neglected. At penetration of the containment wall and at the connection to the steam generator all degrees of freedom were fixed in the finite element model.
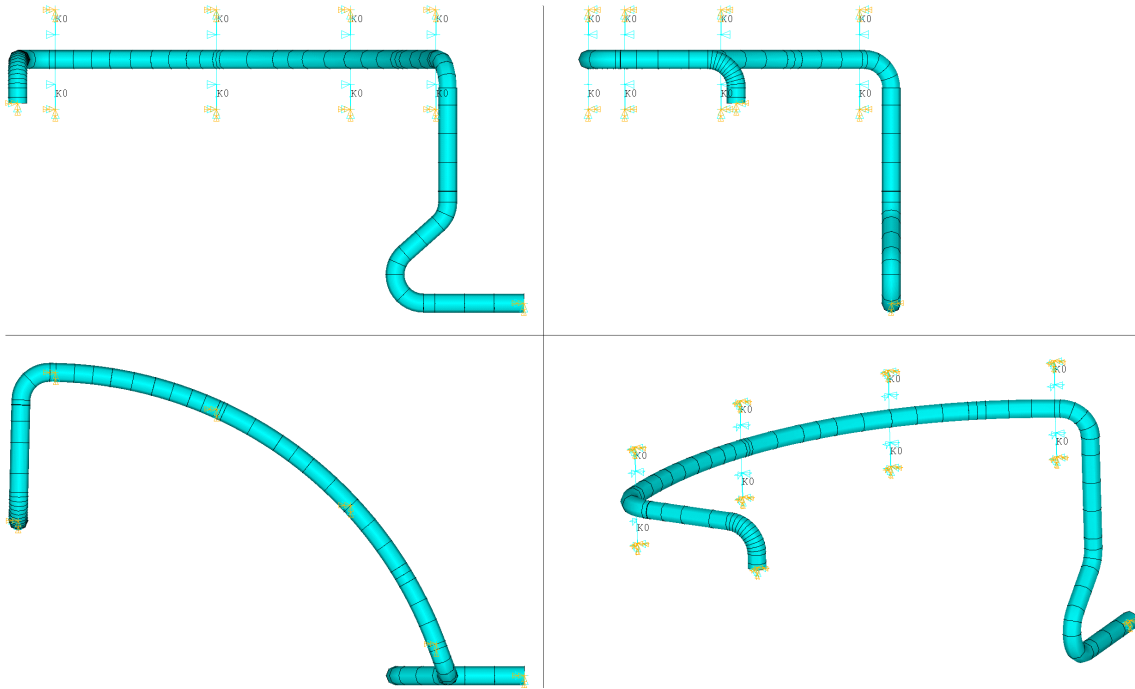
Figure 3.10: Finite element model of TPS.

3.2.3 Analysis of the typical piping system

In the analysis the gap size, c, was equally incrementally changed in all supports, according to

$$c(i) = \frac{0.042}{49}(i - 1) \text{ [m]} \qquad (3.4)$$

where i is the current increment numbers and changes according to

$$i = 1 : 50.$$

In Figure 3.11 the curve that represents the initial gap size is plotted.
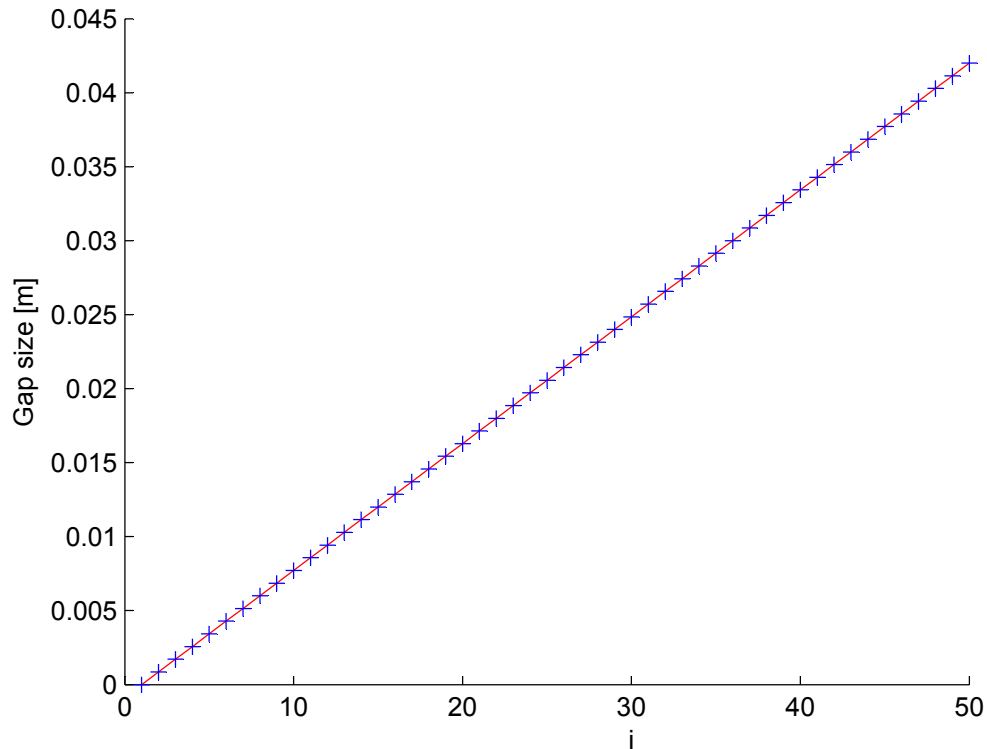
Figure 3.11: Initial gap size versus increments.

Load

The load case acting on the TPS was a pipe break where the break occurred downstream the second anchor point, hence outside the containment wall, see Figure 3.9. The pipe break results in axial forces F_1–F_9 acting on the pipe, see Figure 3.12. See appendix B for plots and tables over force components 1-9, and Section 2.6 for further information regarding the load scenario.

Damping

Equal damping properties as for the SPS.

Time stepping

Equal time stepping scheme as for the SPS.

Assumptions Same assumptions as for the SPS, except that friction between the pipe and its supports always were neglected.

3.3 Validation

In the Swedish nuclear industry, the pipe analysis program Pipestress is widely used. To be able to interpret and compare the results from ANSYS analyses with Pipestress analyses, the dynamic properties of the ANSYS finite element models 3.1.2 and 3.2.2, without the contact elements conta178, are verified against Pipestress models of the same systems.

The verification covers:
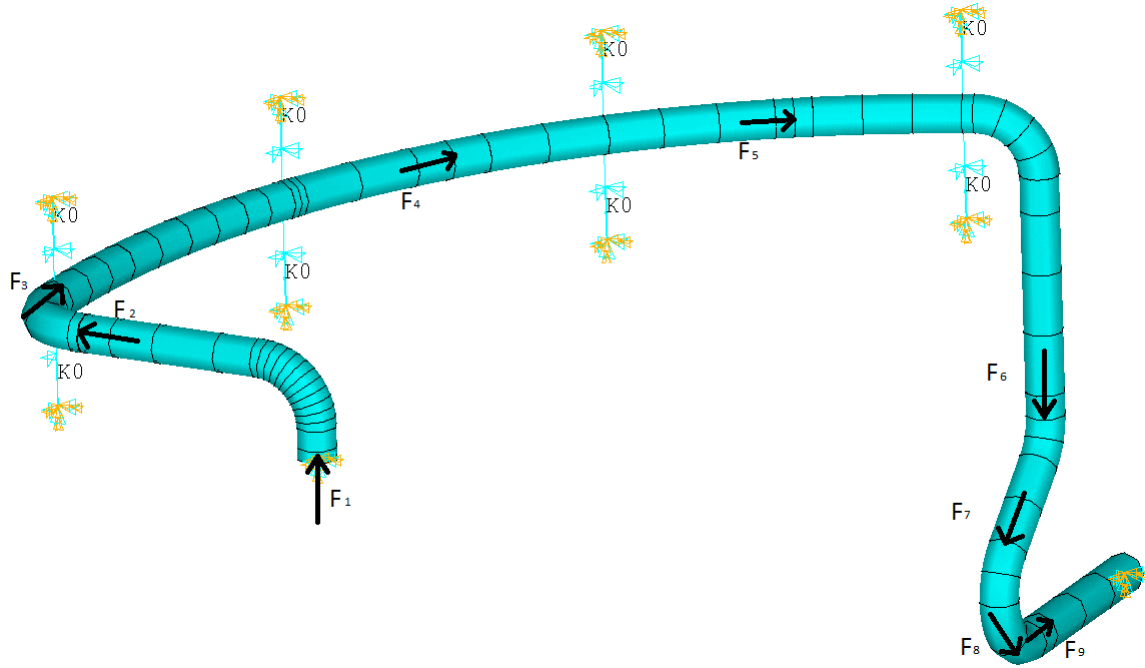
Figure 3.12: Forces acting on TPS due to pipe break.

1. Total mass for the models

2. Eigenfrequencies and eigen modes

3. Dead weight analysis

4. Results from pipe break analysis.

4 Results

This section is divided into two subsections, one for the simplified geometry and one for the typical piping system, see Section 3.1 and 3.2 for information about the piping systems.

4.1 Simplified piping system

Here, the results from the analysis of the simplified piping system are presented. The section is divided into five subsections, Time step evaluation, Contact surface friction, Support stiffness, Gap size and Stiffness approximation.

4.1.1 Time step evaluation

The simplified piping system geom1 v1 was analyzed for different time step lengths according to Equation 3.1. The system was analyzed with a 15 second time history load. The first analysis, with a 1ms time step, took four minutes to complete on a dual core computer. The thirteenth and last analysis, with a 0.0077ms time step, took 5 hours and 44 minutes. Smaller time steps were not considered in this thesis due to to long calculation time. All analyses were done in two versions, one with a support stiffness of 700 kN/mm (standard stiffness, see Appendix C) and one with 235kN/mm support stiffness. This was to investigate the effect of support stiffness on convergence.

To measure the convergence, the largest reaction peak force, found in support A, was chosen, see right plot of Figure 4.1. The peak force in the figure belongs to the smallest time step. The time step size was then varied and the spike values were recorded. These values can be seen in the left plot of the figure. As can be seen, the peak force is very sensitive to time step variations and the convergence is relatively low but the 700kN/mm curve seems to partly stabilize at the smaller time steps.
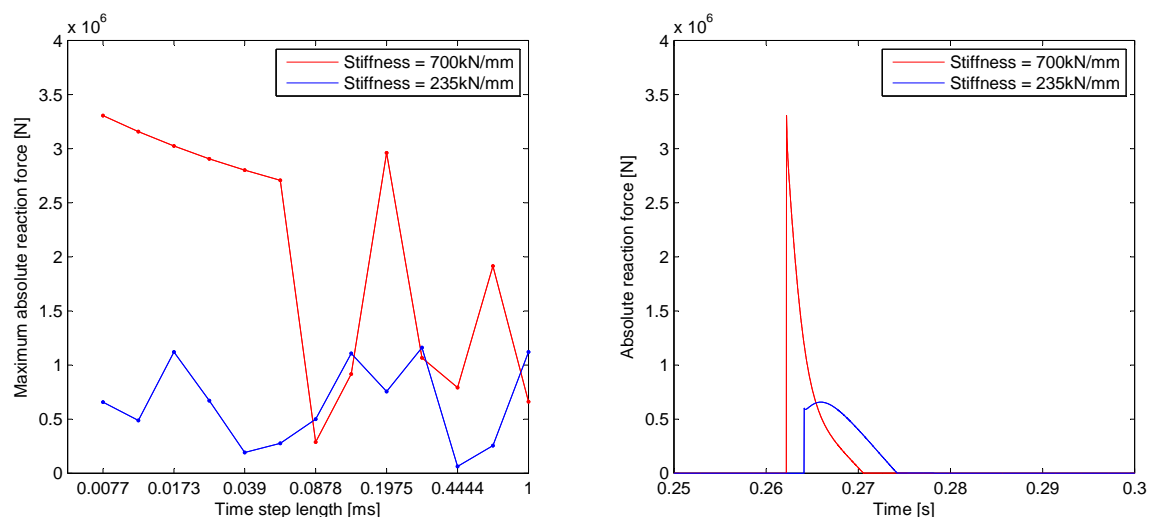
Figure 4.1: Time step size analysis (left figure) of reaction peak force in support A (right figure) for two different support stiffnesses.

Figure 4.2 shows a convergence plot, similar to Figure 4.1, but instead of reaction force it shows the effective stress according to Tresca of a element near support A. The variation

with time step size is very small and it converges much better than the corresponding reaction force.
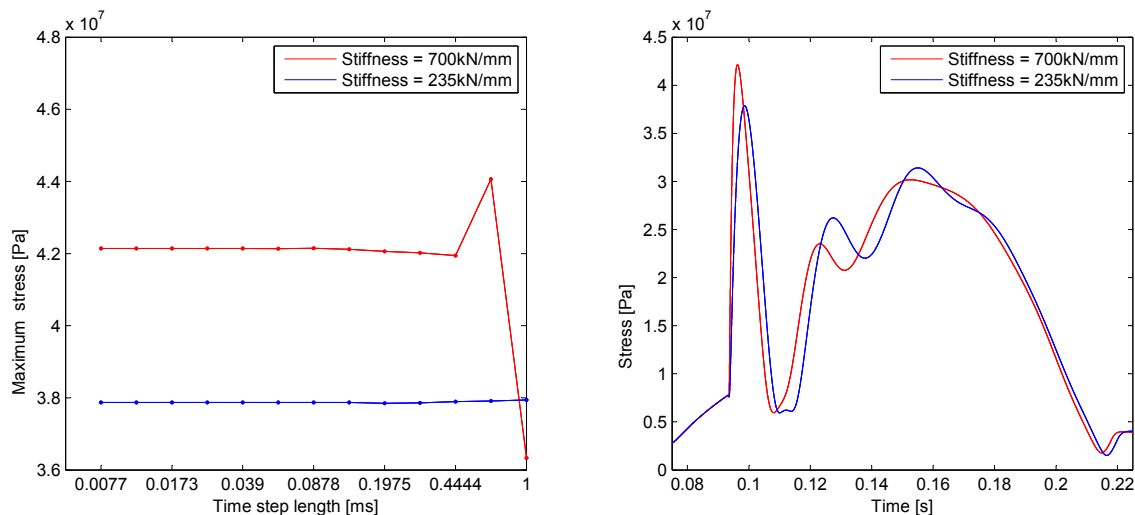
Figure 4.2: Time step size analysis (left figure) of stress intensity in pipe element closest to support A (right figure).

Figure 4.3 shows the same thing as Figure 4.2 but for the element located close to support B. This is the element that experiences the largest stress. This stress is relatively slow and the convergence is therefore very good.
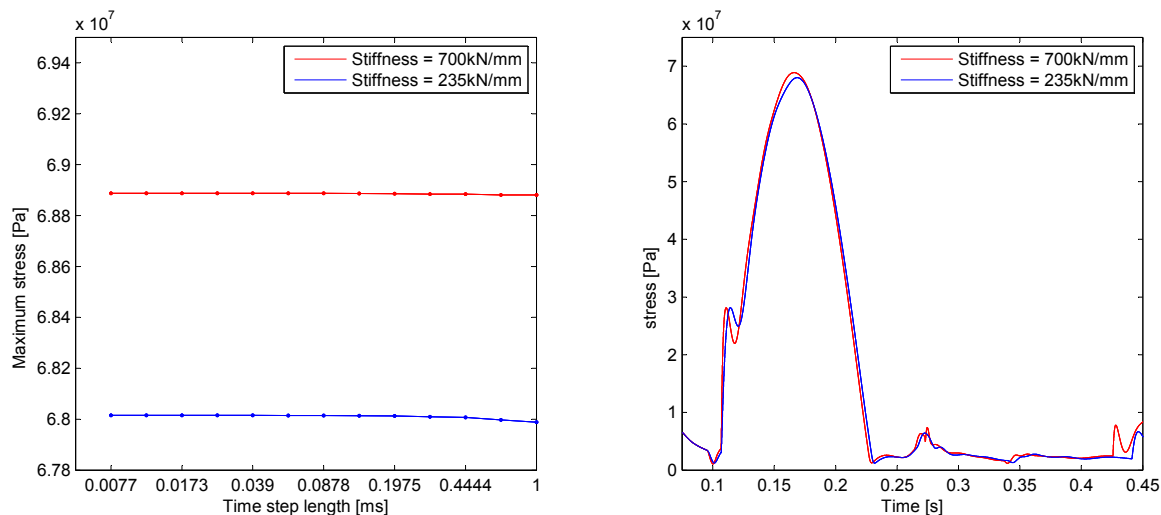
Figure 4.3: Time step size analysis (left figure) of stress according to Tresca in pipe element closest to support B (right figure).

4.1.2 Contact surface friction

As described in Section 3.1.3.2, analyses with friction in the contact surface between the support and the pipe were conducted. The purpose with these analyses were to investigate the influence on the piping system and its supports when friction in the contact surface between the pipe and supports was accounted for. Three different gap sizes were chosen, namely, 15.01 mm, 68.29 mm and 257.1 mm. The selection of those gap sizes was based

on maximum support deformation. Hence each of the selected cases corresponds to a local maximum in support deformation in the contact normal direction during a pipe break load case, see Figure 4.4.
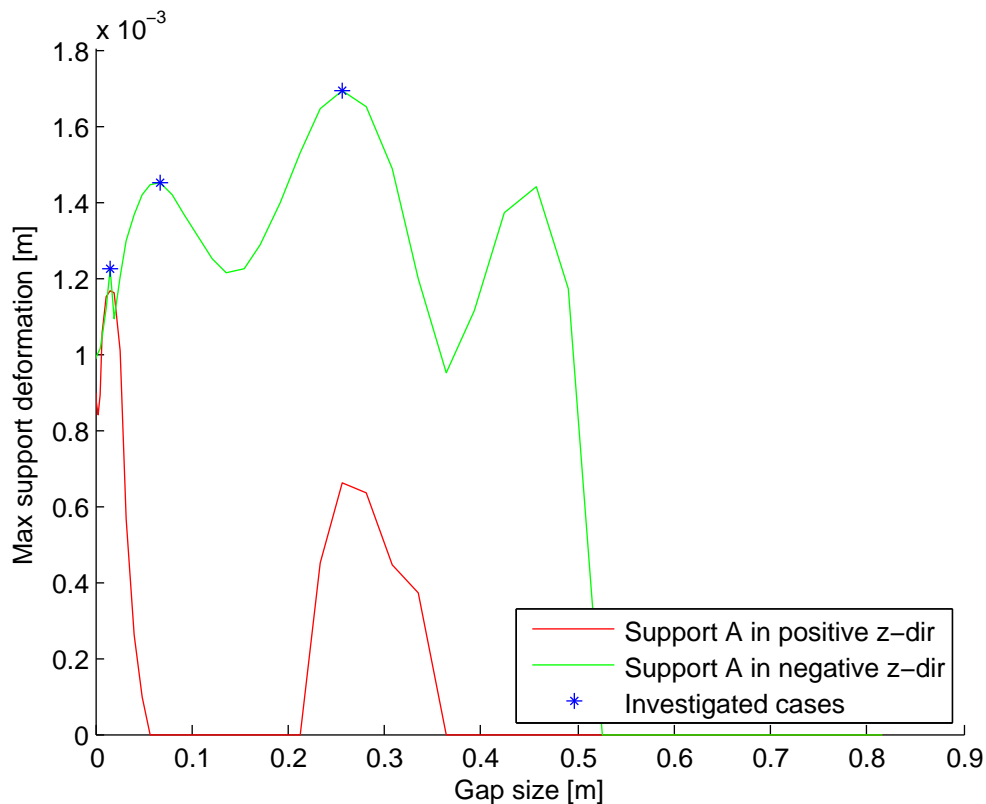
Figure 4.4: Max support deformation in the normal-direction plotted versus gap size, selected cases for friction analysis.

The contact was modeled using the Lagrange multiplier method in the contact normal-direction and the Penalty method in the contact tangential (friction)-direction.

The stresses in the piping system were generally equal or slightly lower when friction was taken into account. Maximum stress in the pipe occurred at the same location, both with and without friction in the contact surfaces. See Figure 4.5-4.7 for plots over stress versus time in the elements close to supports A and B for the three different cases.
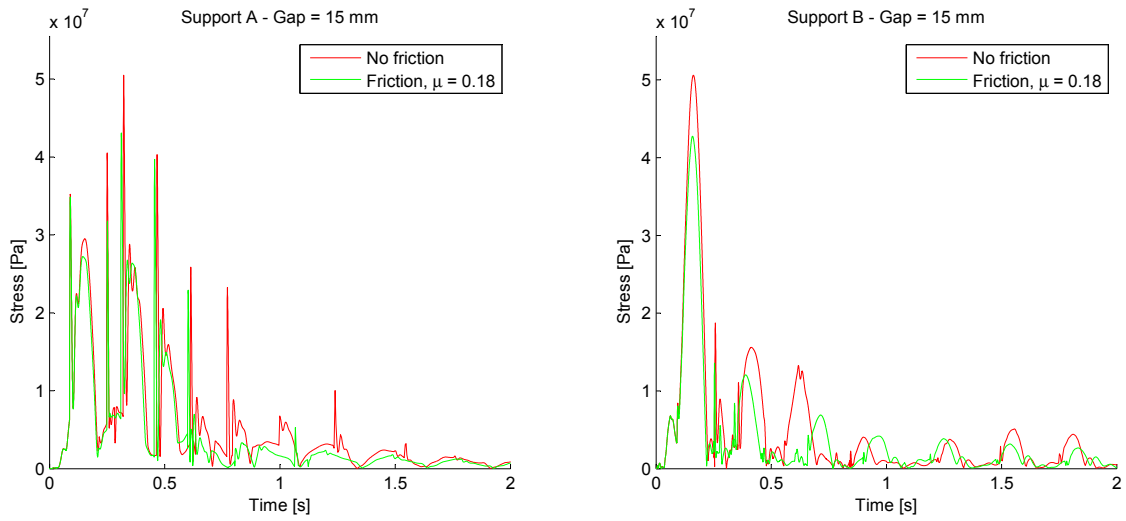
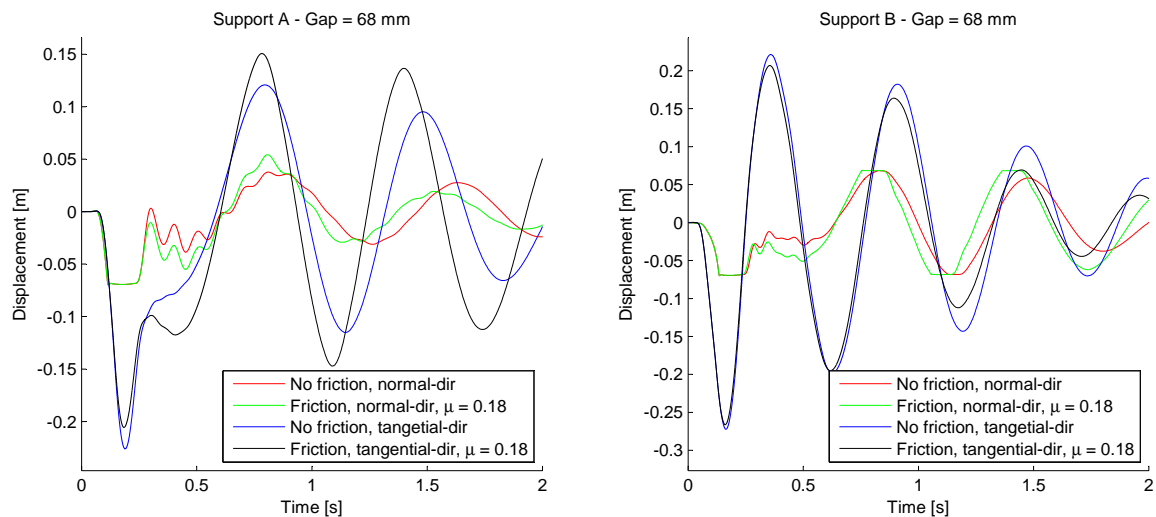Figure 4.5: Stress versus time in pipe elements close to supports A and B, with and without friction, gap = 15 mm.
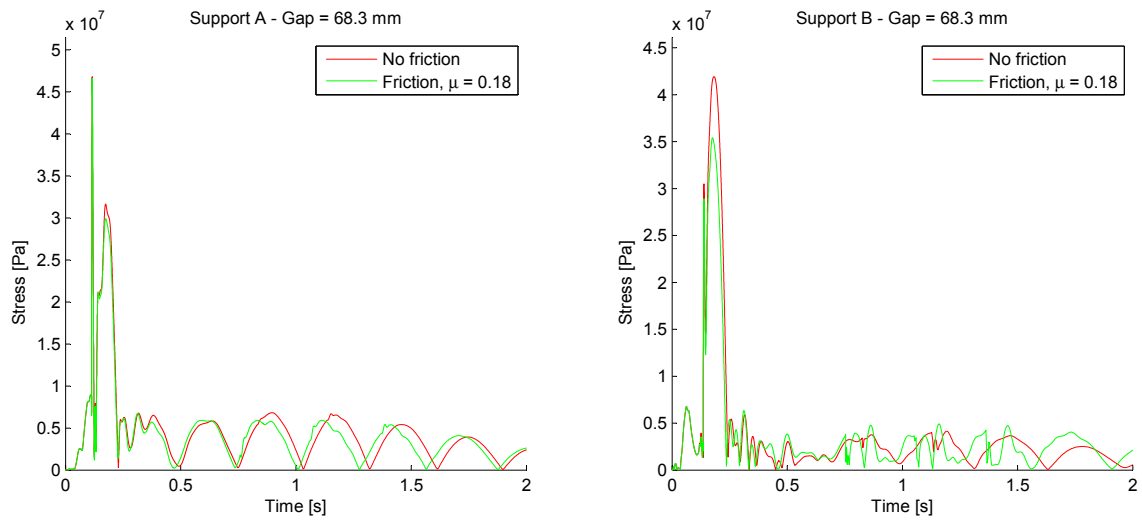
Figure 4.6: Stress versus time in pipe elements close to supports A and B, with and without friction, gap = 68 mm.
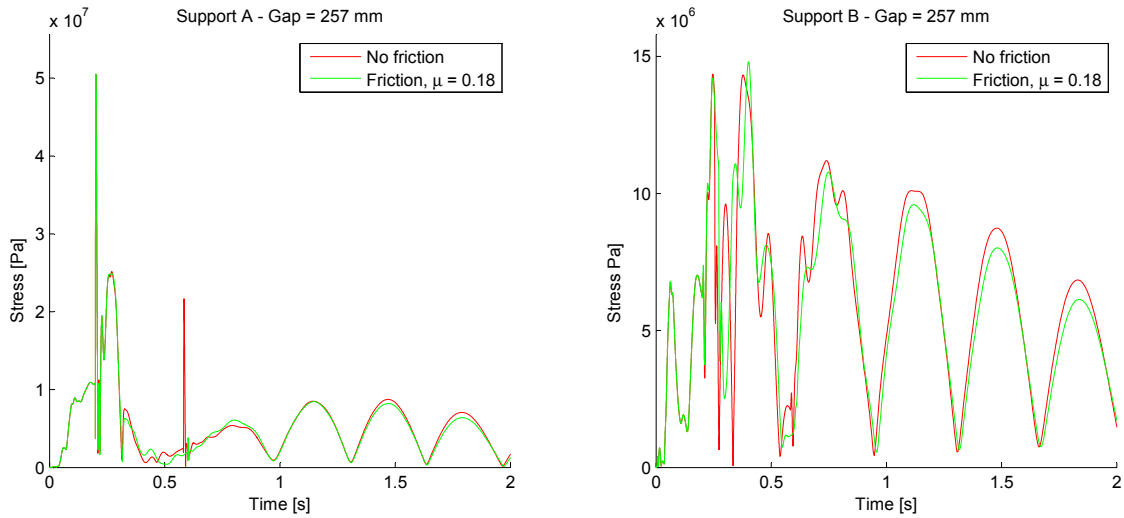
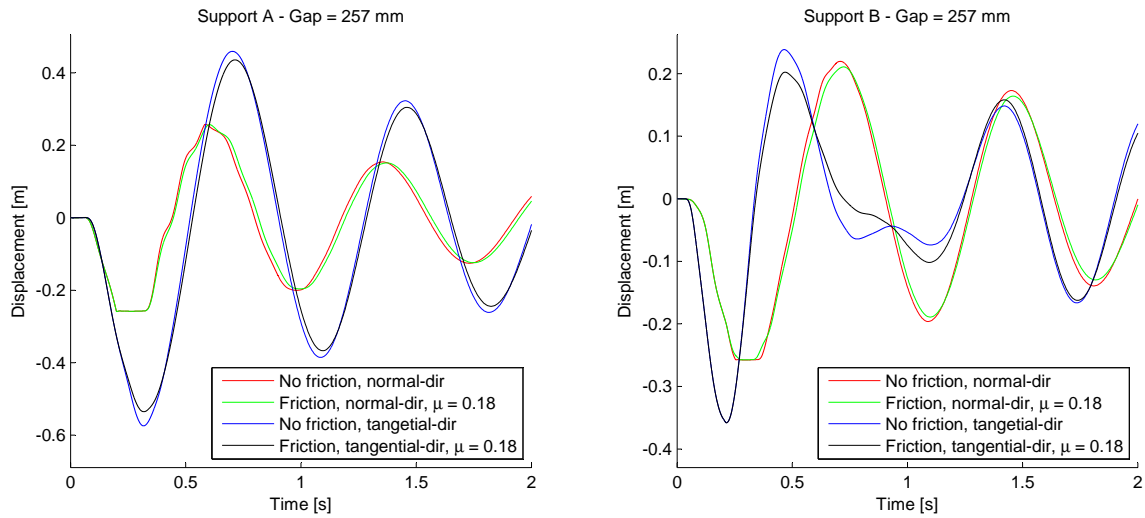Figure 4.7: Stress versus time in pipe elements next to support A and B, with and without friction, gap = 257 mm.

In Figure 4.8 -4.10, the reaction forces of the two supports are shown. Reaction forces normal to the contact plane and in the case when friction is accounted for also additional tangential forces are plotted.
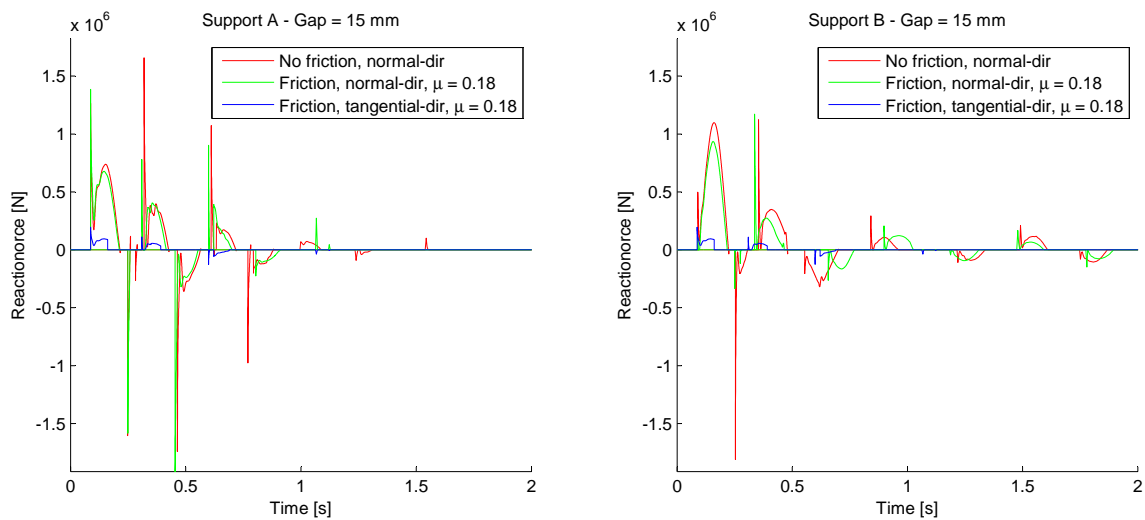
Figure 4.8: Force versus time in pipe elements next to support A and B, with and without friction, gap = 15 mm.

Generally slightly higher support reaction forces were obtained in the case was no friction on the contact surface were assumed.
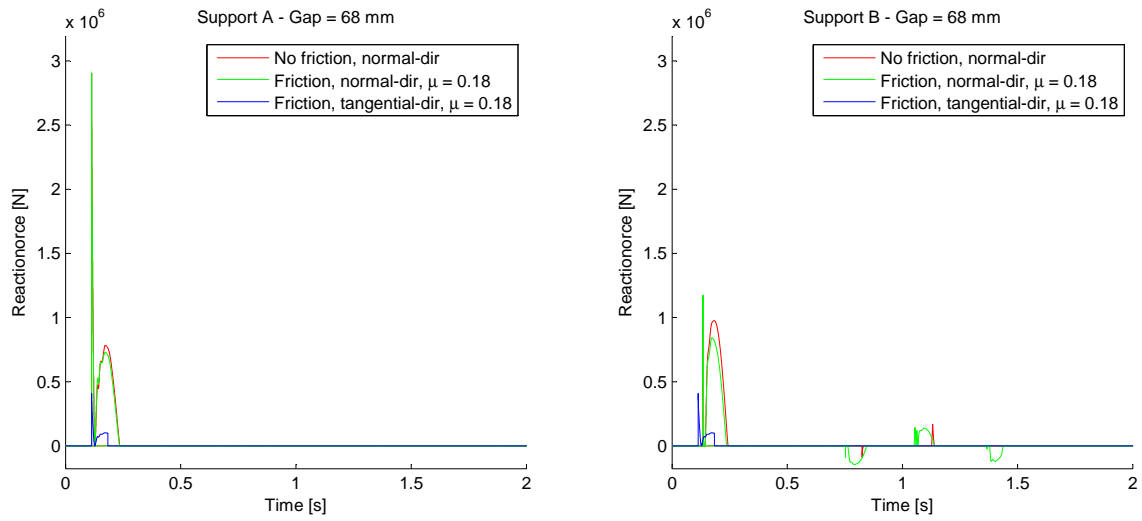
Figure 4.9: Force versus time in pipe elements next to support A and B, with and without friction, gap = 68 mm.
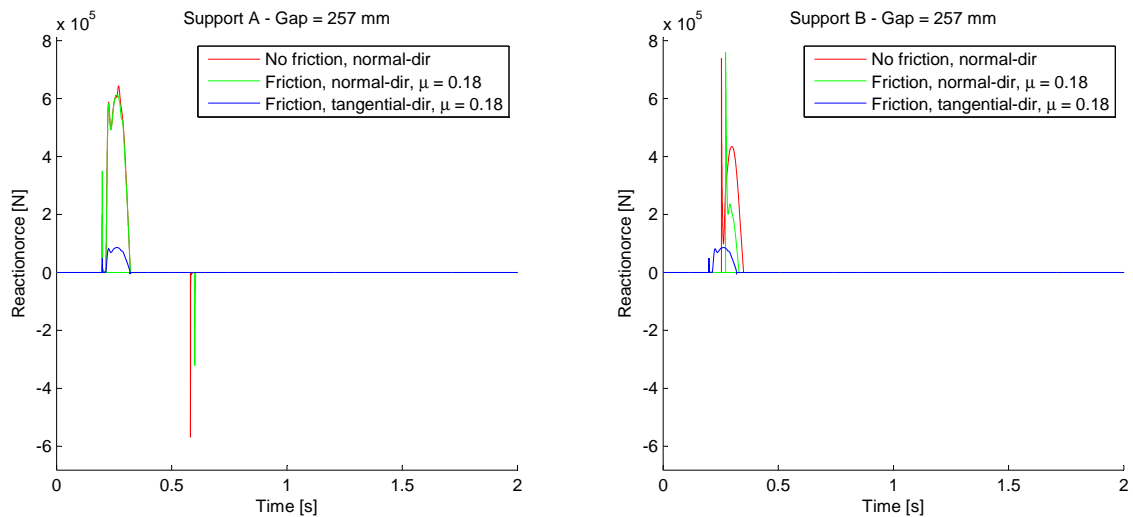
Figure 4.10: Force versus time in pipe elements next to support A and B, with and without friction, gap = 257 mm.

In Figure 4.11-4.13 the time history of the displacement in normal and tangential direction of the pipe nodes located next to the supports A and B is plotted, for the three different cases.
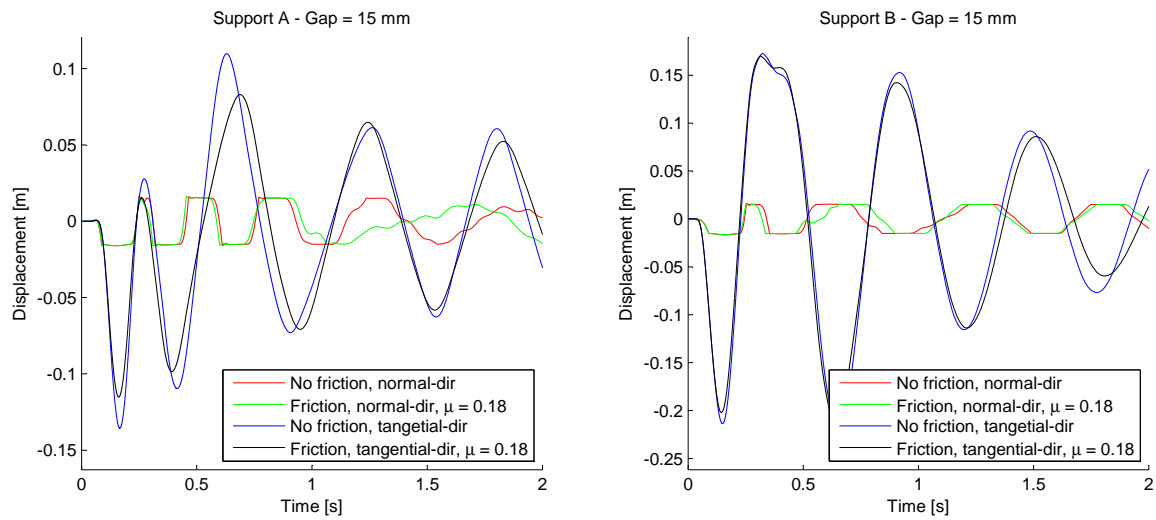
Figure 4.11: Displacement versus time in pipe elements next to support A and B, with and without friction, gap = 15 mm.

Figure 4.12: Displacement versus time in pipe elements next to support A and B, with and without friction, gap = 68 mm.

Figure 4.13: Displacement versus time in pipe elements next to support A and B, with and without friction, gap = 257 mm.

4.1.3 Support stiffness

In Figure 4.14 one can see a time history plot of the reaction forces at support A with and without a gap. A standard gap stiffness is used and there is clearly a large peak force at the second impact. The reaction force for the support without a gap does not change much with varying support stiffness and will therefor only be showed with the standard stiffness. A closer view of the peak force can be seen in Figure 4.15. Here it is shown for five values of support stiffness and the same gap size, 25.7mm. All the points in the figure are values obtained from the analysis, so the horizontal distance between them is the time step size. For the higher stiffnesses, the first two spike values are far apart. This could unfortunately not be amended by refining the time steps, see Section 3.1.3.1. When the support stiffness is lowered from 700kN/mm to 235 kN/mm, the spike characteristics disappear. The first value of the spike is no longer the highest value of the spike.

Figure 4.16 shows the two first impacts of the pipe against the support. This illustrates how the support stiffness affects different kinds of forces. The first impact reaction force, is relatively slow and long lasting. The second impact, reaction peak force is fast, short lasting and largely affected by the support stiffness. The effective stress (according to Tresca), of the pipe element located close to support A, is shown in Figure 4.17. It is plotted for the exact same time span as in Figure 4.16. When comparing these plots one can see that the first, long lasting, force has the largest affect on the pipe stress.
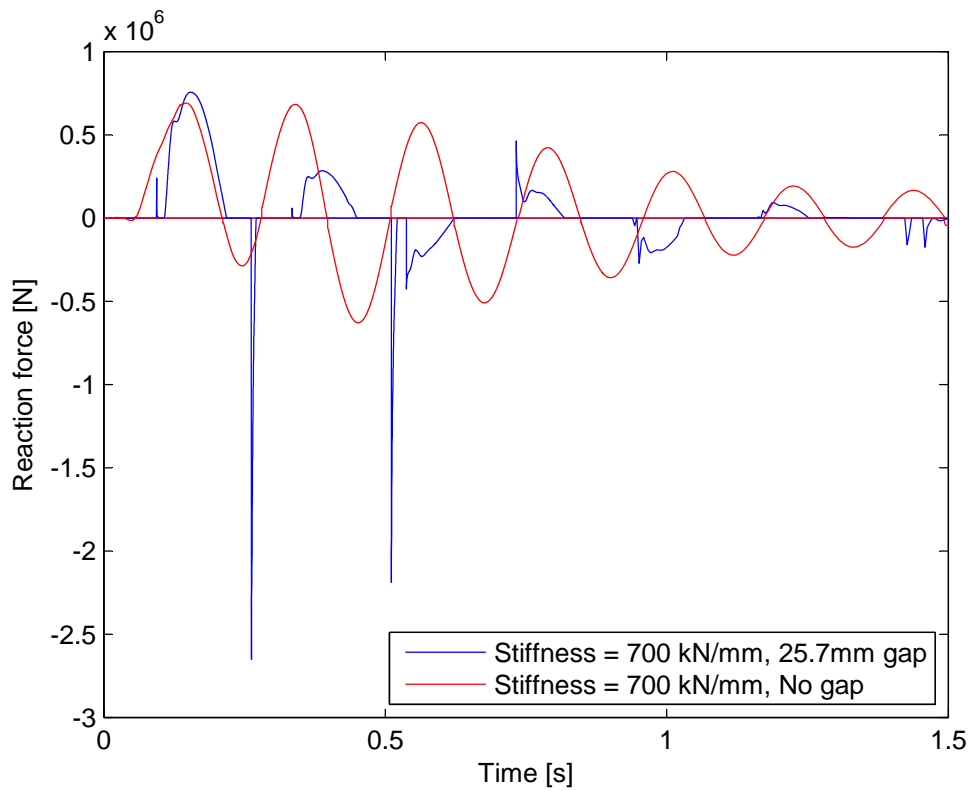
Figure 4.14: Support reaction force with and without a gap
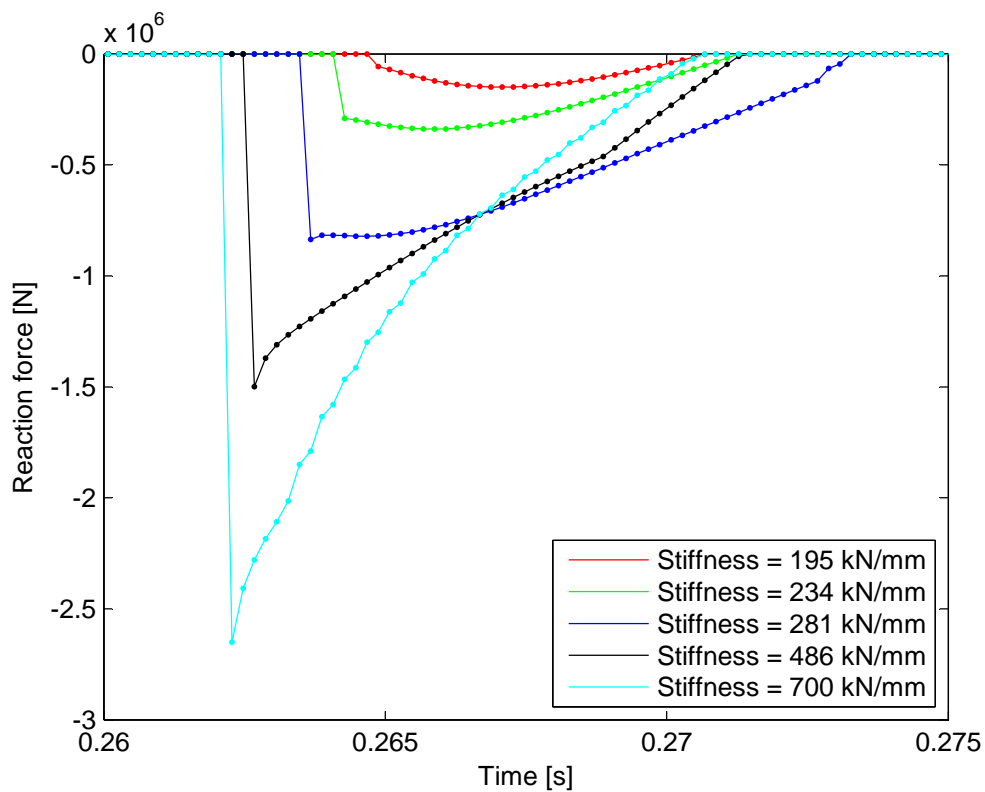
Figure 4.15: Support reaction peak force
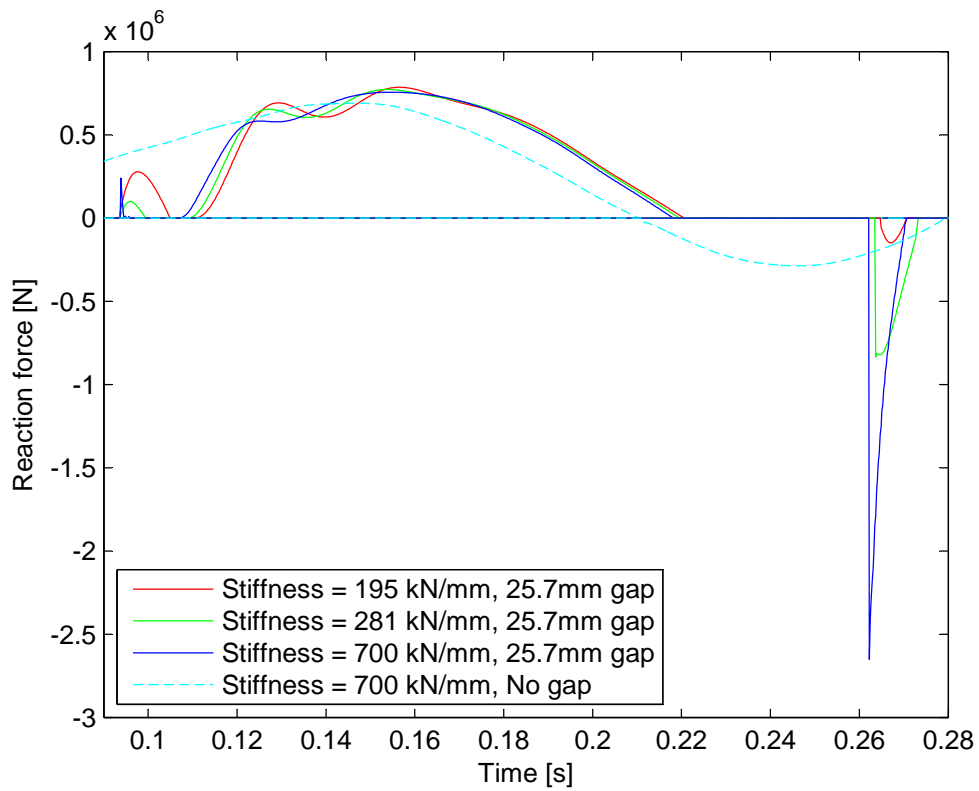
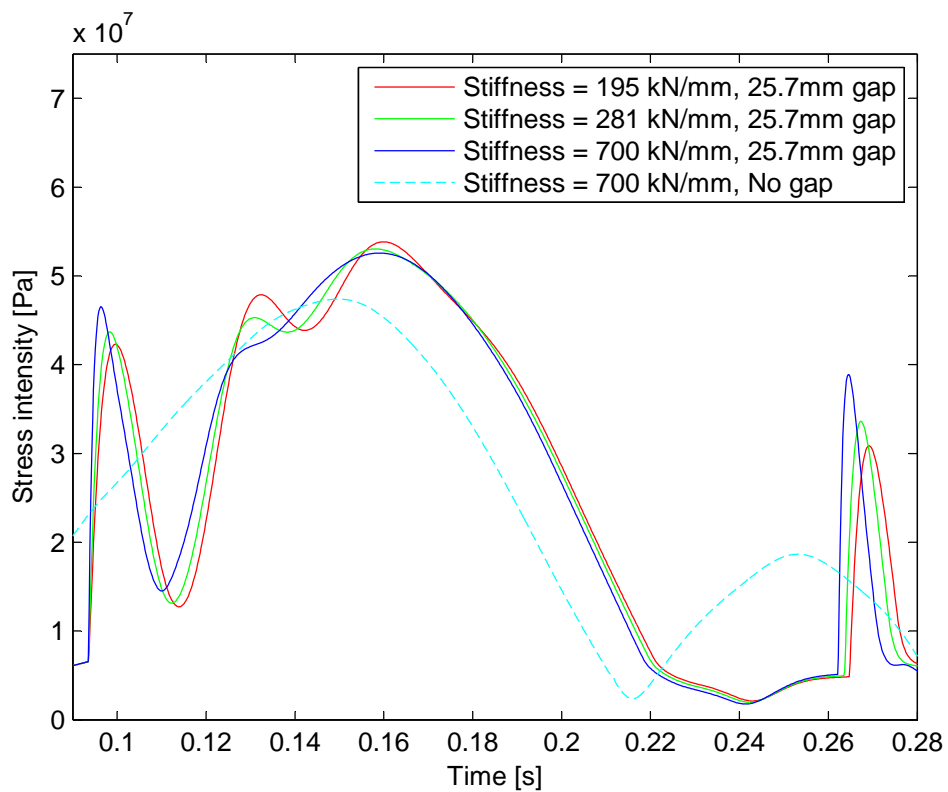Figure 4.16: Support reaction force, first two impacts

Figure 4.17: Pipe stress, first two impacts

4.1.4 Gap size

In this section the results from the analysis introduced in Section 3.1.3.4 is presented. During the analysis the piping system endured a pipe break time history load. The essence of the analysis was the incremental change of the gap size between the pipe and it supports. All four version of geom1, $v_1 - v_4$, were studied in the analysis.

In Figure 4.18 the maximum stress occurring for each gap size in the four different versions of geom1 are shown. Note that the location of the maximum stress, in the pipe for each gap size, may change between the increments.
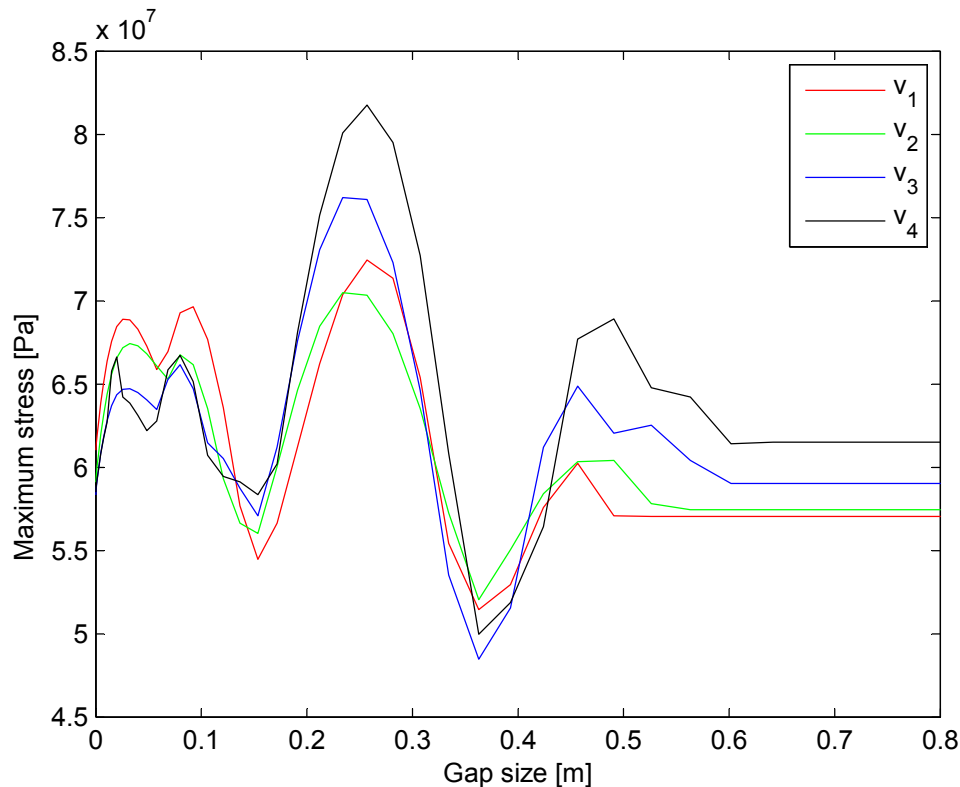
Figure 4.18: Maximum pipe stress versus gap size, for all versions of geom1.

Compared with Figure 4.18 where no certain elements were investigated, the plot in Figure 4.19 follows the maximum stress response for each gap size of four different elements in geom1. *Element* 1 is situated at the left anchor point, *Element* 146 is situated at support A, *Element* 206 and *Element* 210 are near support B. The dotted line denoted *Maximum* is equal to the one denoted v_1 in Figure 4.18, hence, v_1 is the maximum effective stress occurring in the pipe.

Maximum reaction forces in support A for each gap size in both positive and negative z-direction are shown in Figure 4.20 and in Figure 4.21. Since the maximum value of the reaction force for each gap size often corresponds to a spike value, also the maximum support deformation of support A is included in the figures.
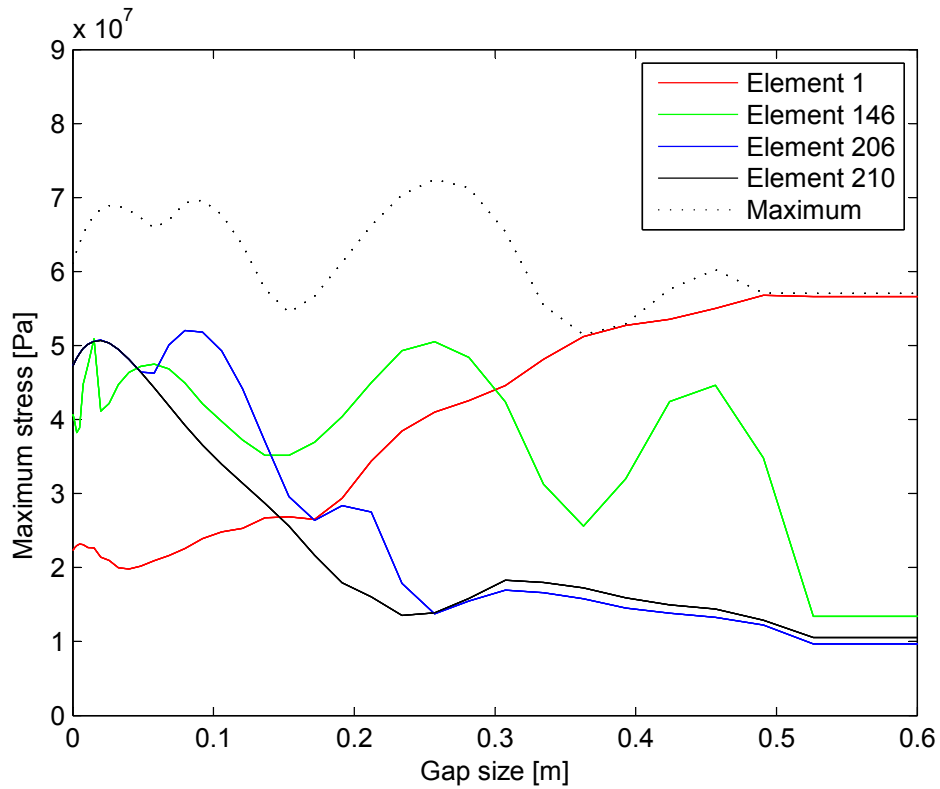
Figure 4.19: Maximum pipe stress for four elements versus gap size together with the maximum stress for all elements, for version v_1 of geom1.
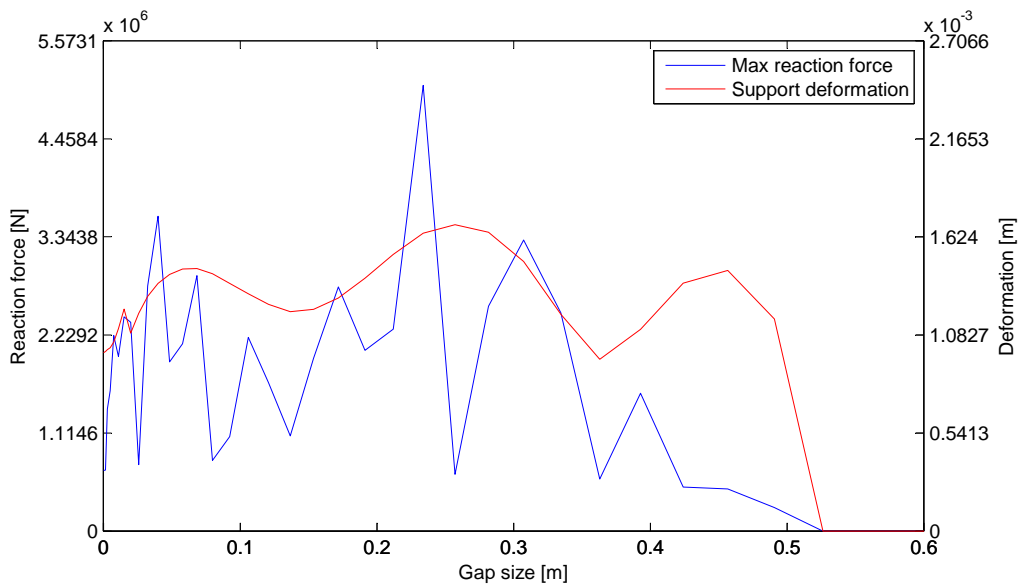

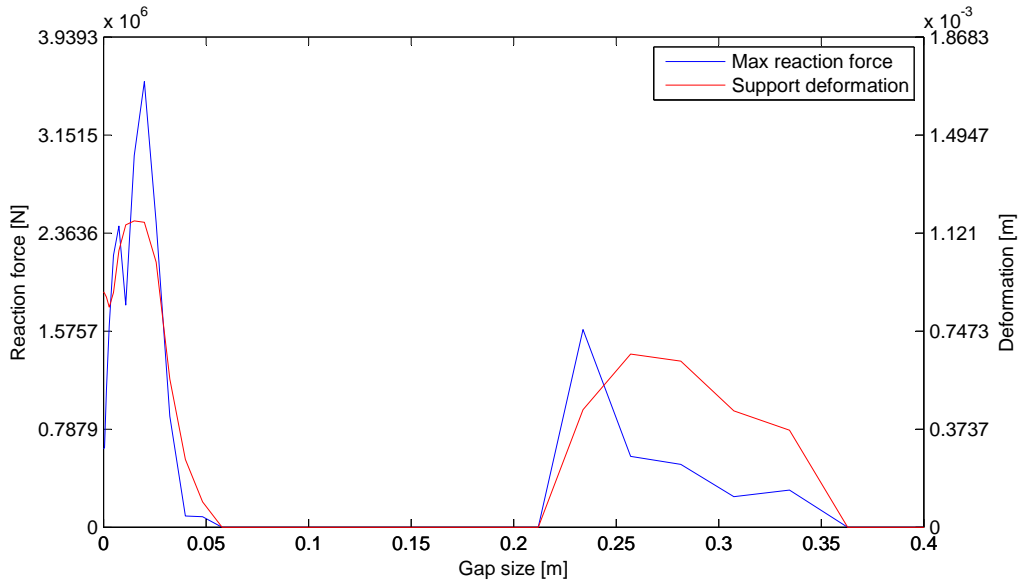Figure 4.20: Maximum reaction force, and maximum deformation of support A in negative z-direction.

Figure 4.21: Maximum reaction force, and maximum deformation of support A in positive z-direction.

In Figure 4.22 the local maximum support deformation and maximum stress are marked, hence those points correspond to gap sizes where the supports and the pipe are exposed to high loads.

The time history results associated to those gap sizes for support A and B in geom1 v_1 are presented in the following figures: 4.23, 4.24. Both reaction force and stress are shown in the figures. The gap sizes corresponding to the highlighted points in Figure 4.22 are compared to results with no gap in Figure 4.25 and 4.27. Standard support stiffness are used in both cases.
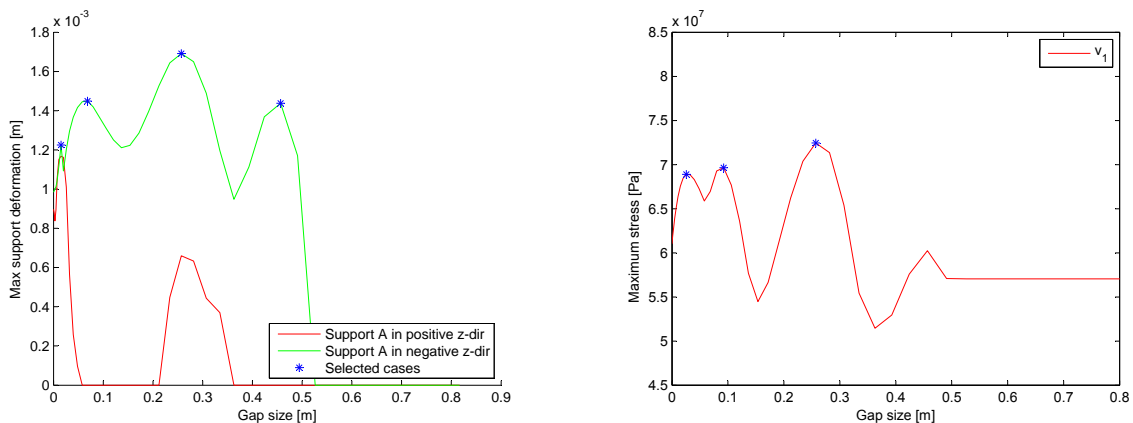
Figure 4.22: Max support deformation and max stress versus gap size in geom1 v_1, investigated cases.
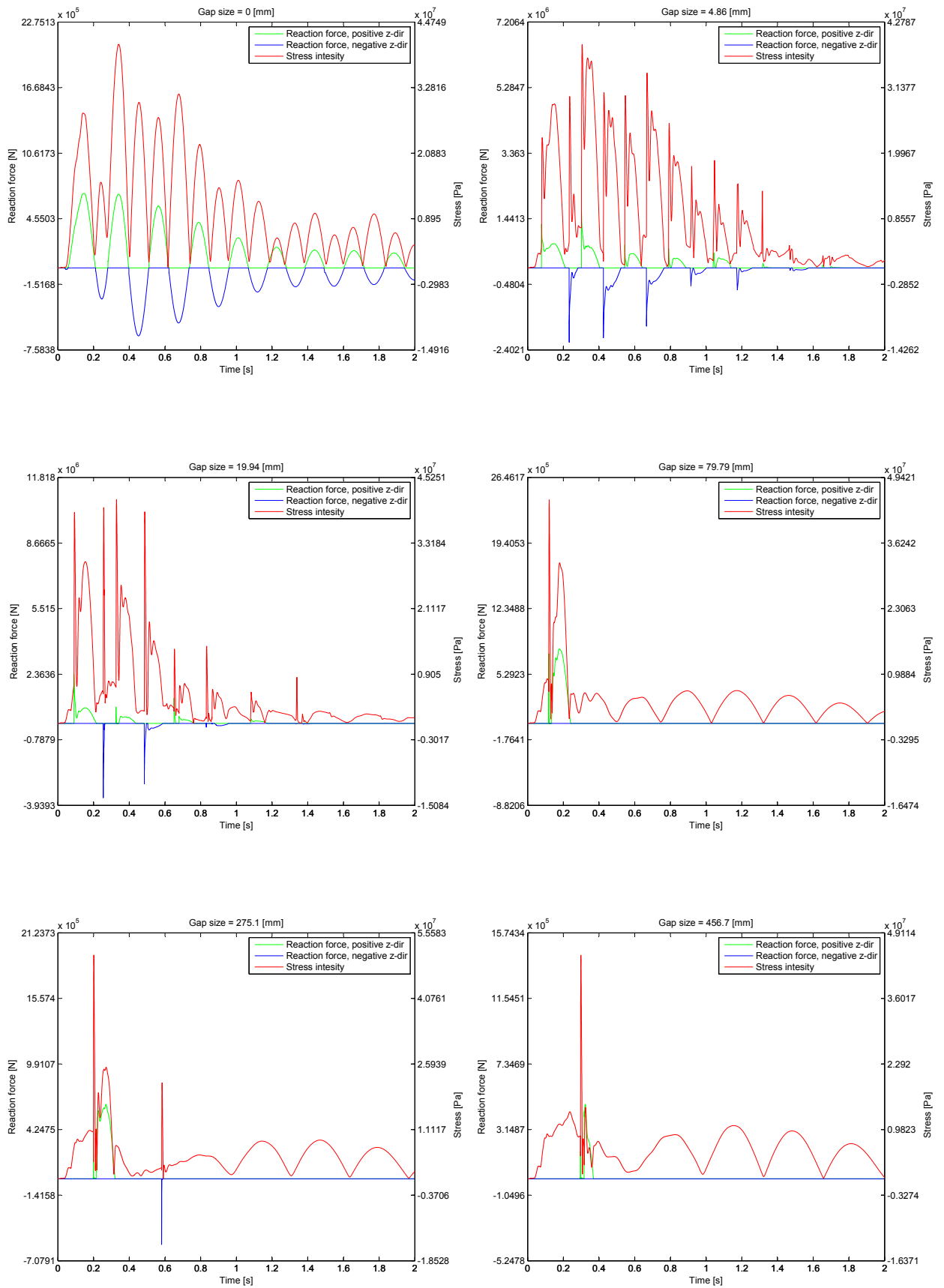
Figure 4.23: Time history results, stress and reaction force at support A.
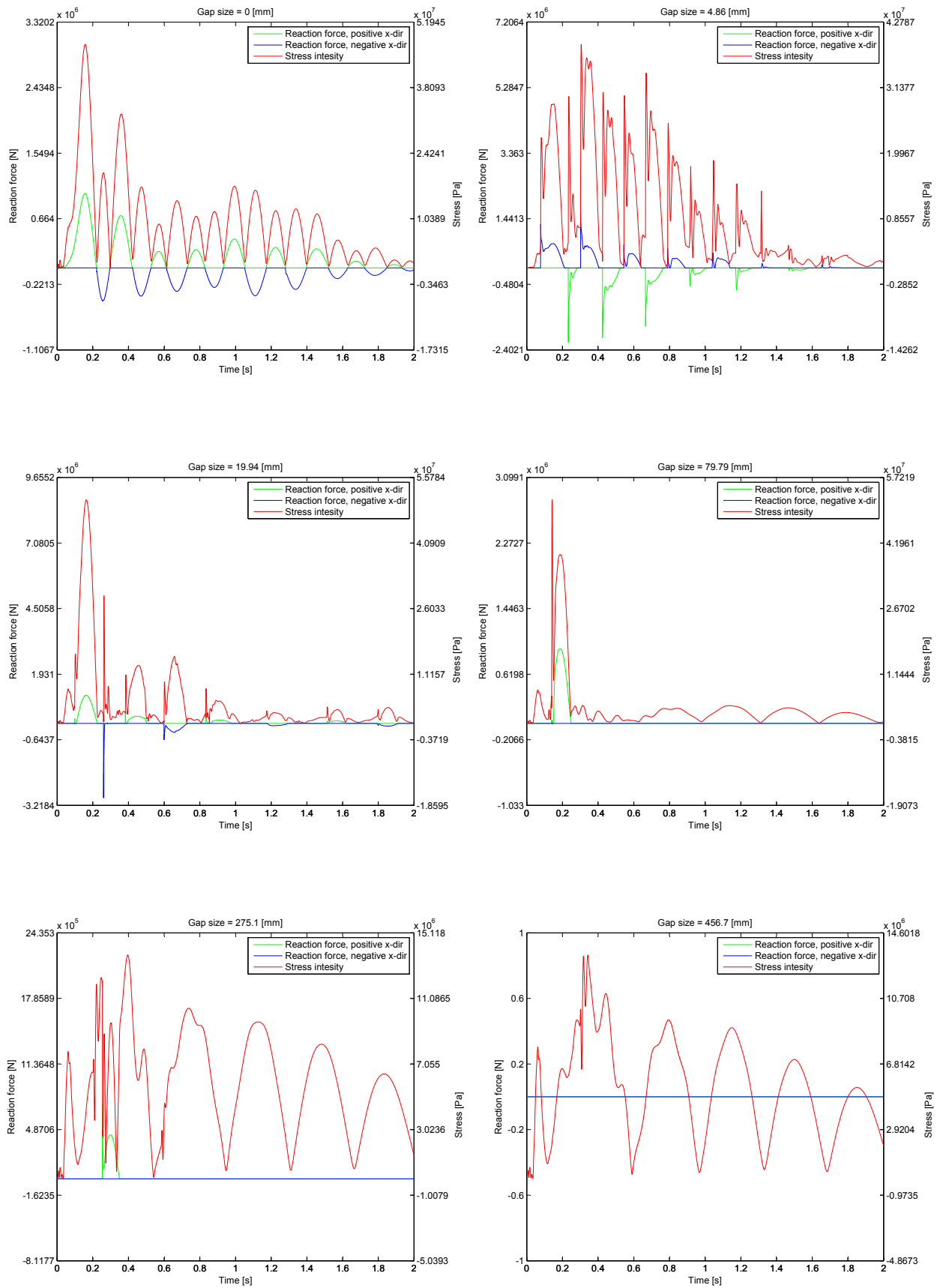
Figure 4.24: Time history results, stress and reaction force at support B.
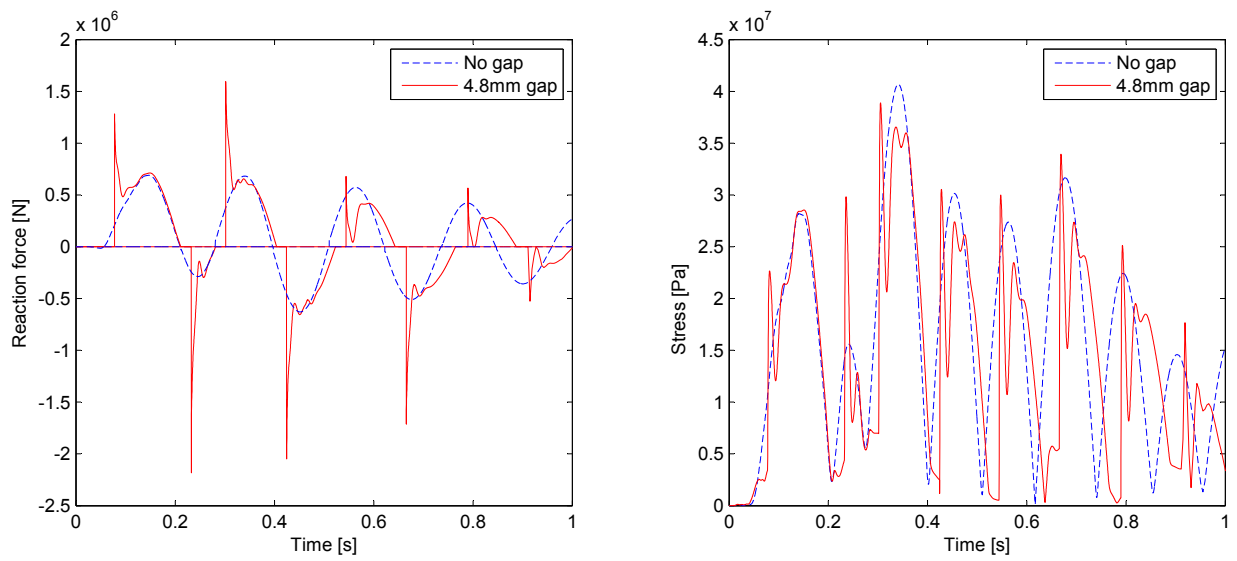
Figure 4.25: Time history of effective Tresca stress and force in support A, gap = 4.86 mm.
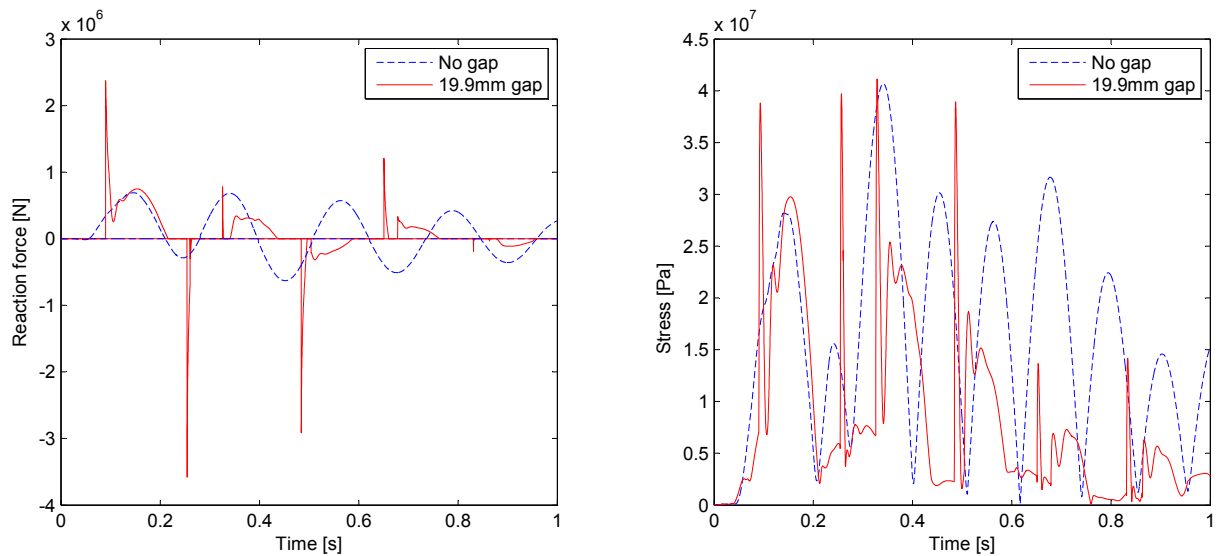

Figure 4.26: Time history of effective Tresca stress and force in support A, gap = 19.91 mm.
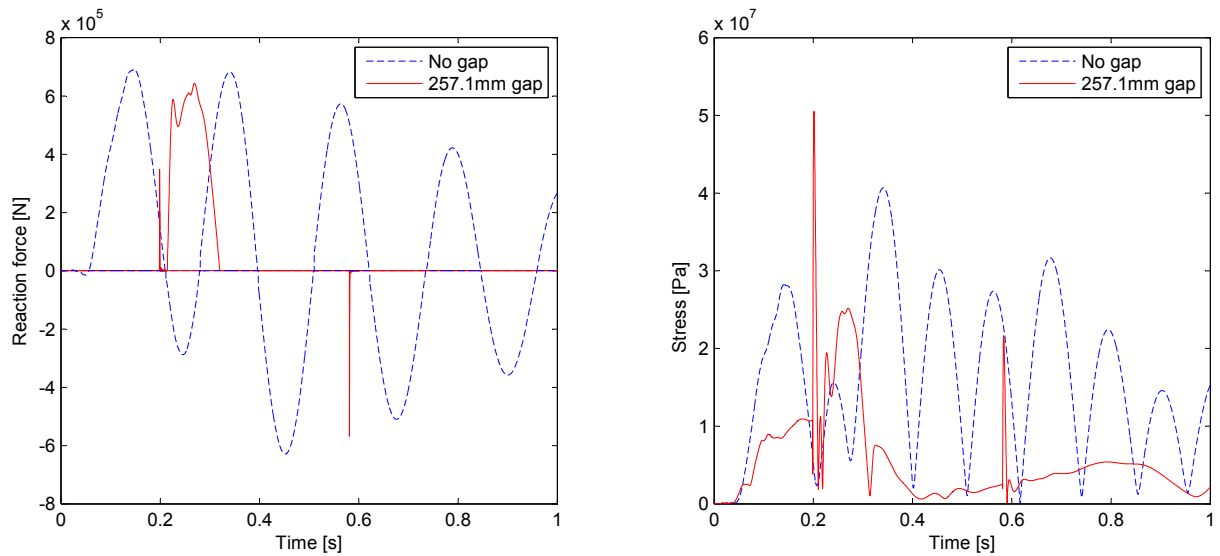
Figure 4.27: Time history of effective Tresca stress and force in support A, gap = 257.1 mm.

As previously mentioned, the time history of the reaction force often shows spike characteristics, for example displayed in Figure 4.26. The reaction force closely related support deformation is compared to the reaction force in Figure 4.28 and 4.29.
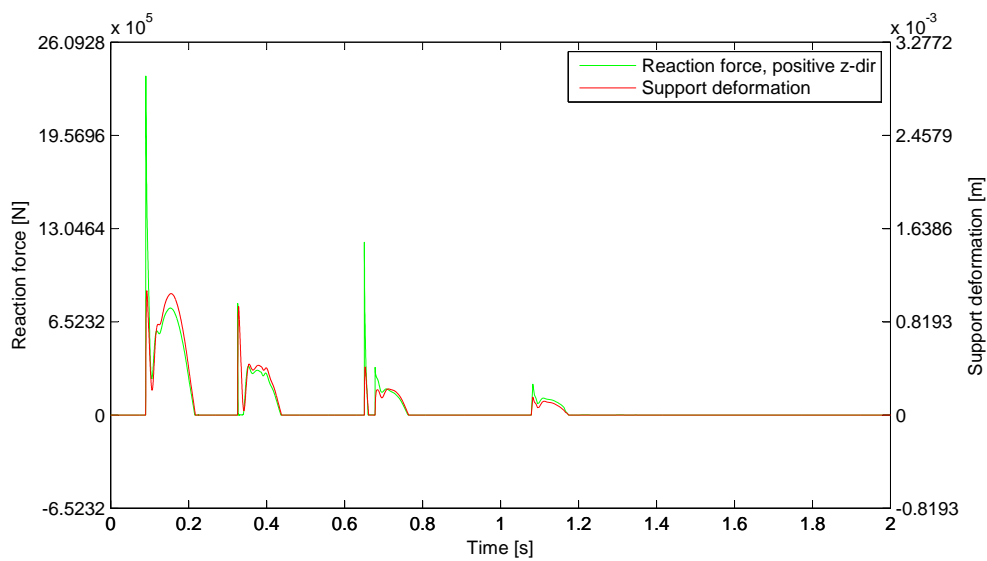
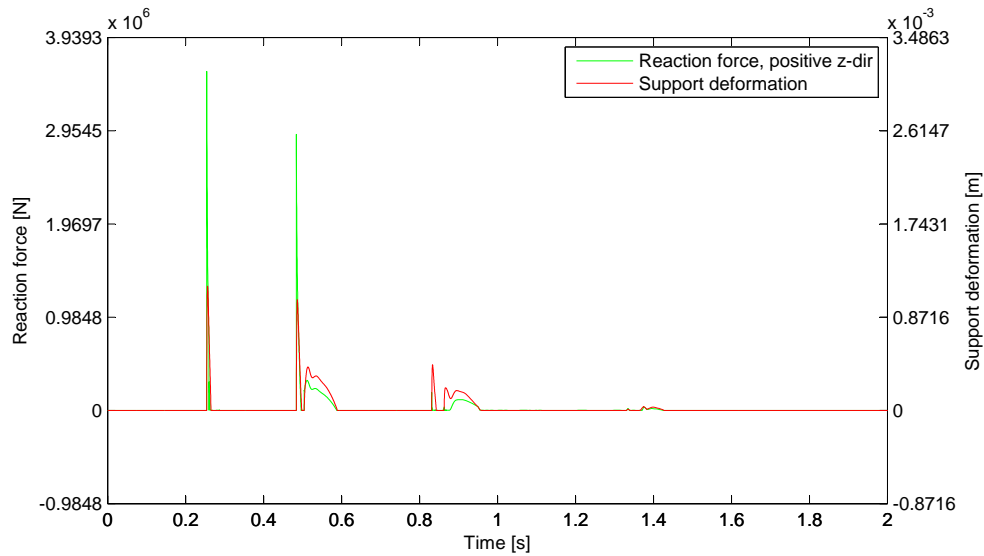Figure 4.28: Time history of reaction force in negative z-direction and support deformation in support A, gap = 19.91 mm.

Figure 4.29: Time history of reaction force in positive z-direction and support deformation in support A, gap = 19.91 mm.

4.1.5 Stiffness approximations

It was investigated if one could approximate the behavior of a gap support by varying the stiffness of support without a gap. In Figure 4.30 one can see a plot of the reaction force at support A and the stress of an adjacent element. Two systems with standard stiffness were analyzed, one with and one without gaps. Also, a gap system with 21.9kN/mm stiffness was analyzed. A problem that arose was how to measure the correlation between a system with a gap and one without. As can be seen in Figure 4.30, the appearance of the gap and no-gap curves are quite different. If one was to smoothen the curves from the gap analysis, and thereby remove the spikes, the correlation between the two 700 kN/mm curves would be good.
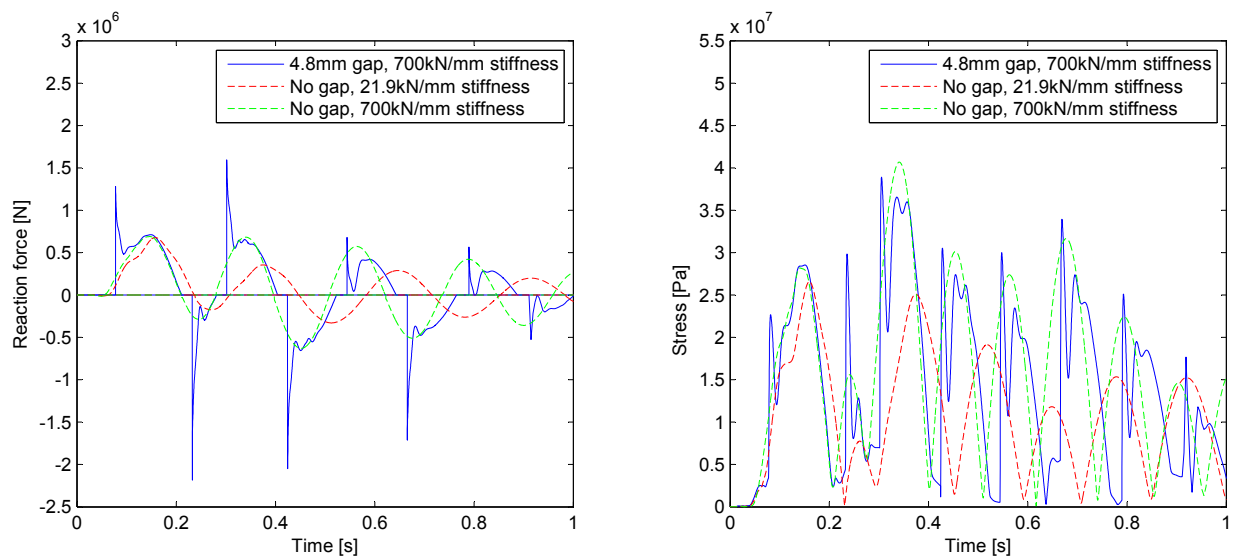

Figure 4.30: Time history of reaction force and stress for different stiffness-gap configurations.

4.2 Typical piping system

In this section the results from the analysis of the TPS is presented. Different support gap sizes were investigated during the analysis.

4.2.1 Support gap size

In this section the results from the analysis introduced in Section 3.2 are presented. During the analysis the piping system endured a transient load case which resembled a pipe break. The essence of the analysis was the incremental change of the gap size between the pipe and its supports.

In Figure 4.31 the maximum stress occurring for each gap size in the pipe is shown. Note that the location of where the maximum stress occurs in the pipe for each gap size may change between the increments. The focus in this section will be on the gap sizes corresponding to local stress maximums, marked with red stars in the figure.
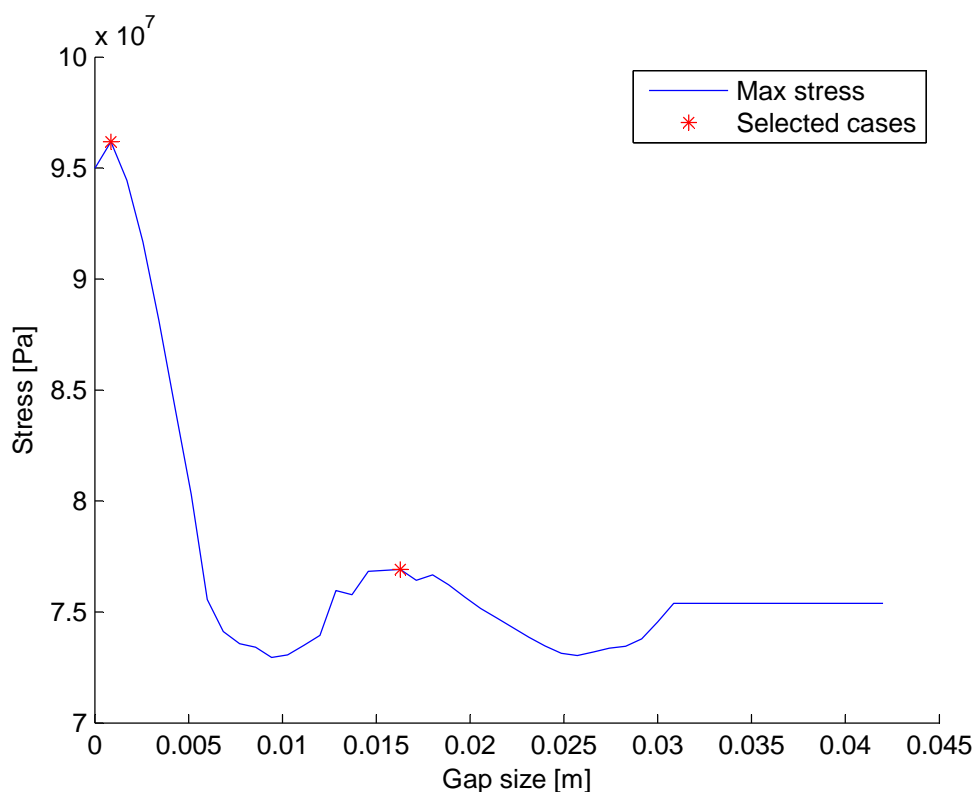

Figure 4.31: Maximum pipe stress versus gap size, red stars show further investigated cases.

Compared to Figure 4.31 where all elements were considered, Figure 4.32 shows the stress in the elements near the supports. *Element* 21 coresponds to support A, *Element* 34 to B, *Element* 50 to C and finally *Element* 54 to D.
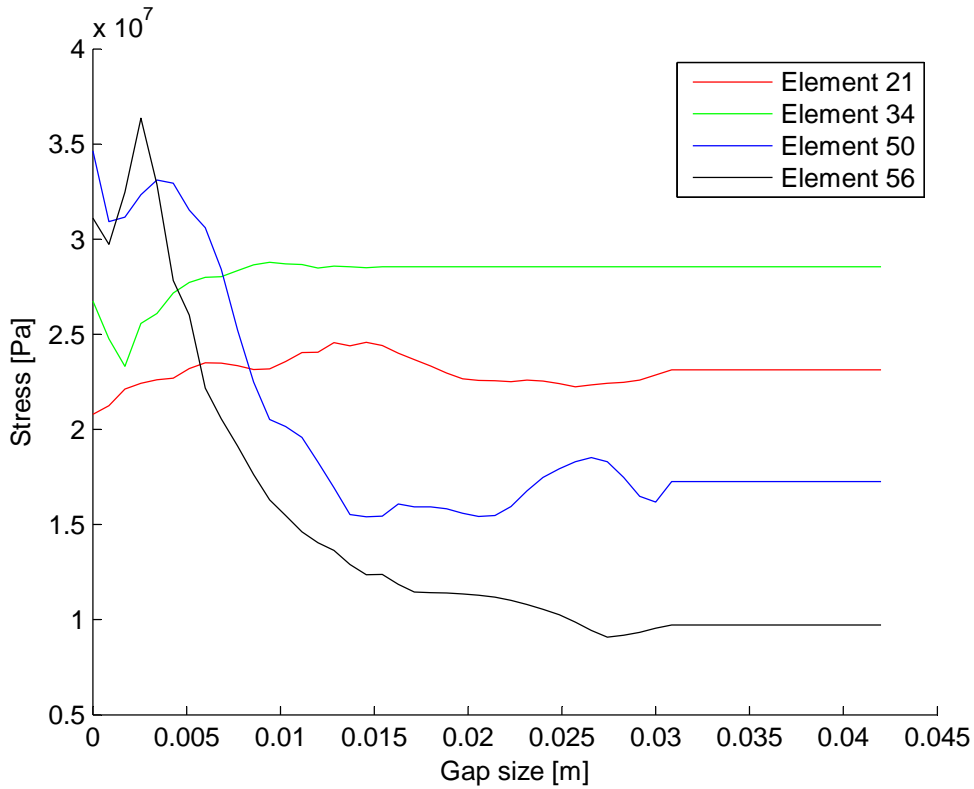
Figure 4.32: Maximum pipe stress versus gap size in elements near the supports.

The time history results associated to those gap sizes for support A - D are presented in the following figures: 4.33 - 4.36. Both reaction force and stress are shown in the figures.
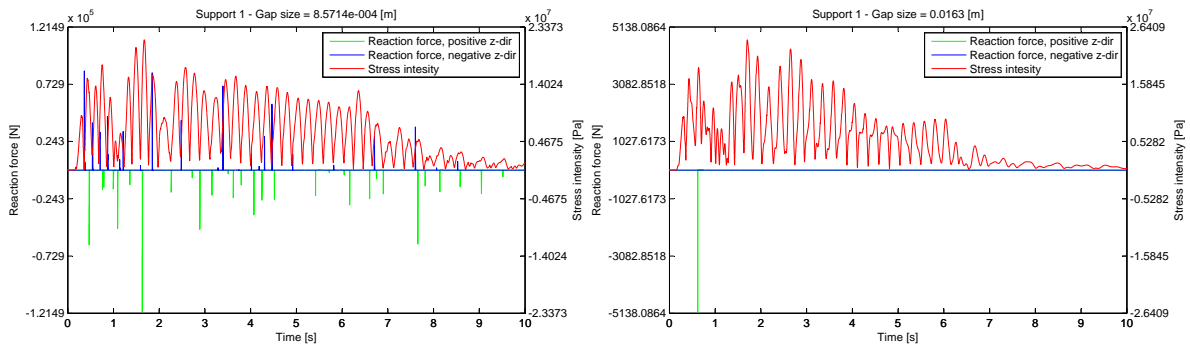

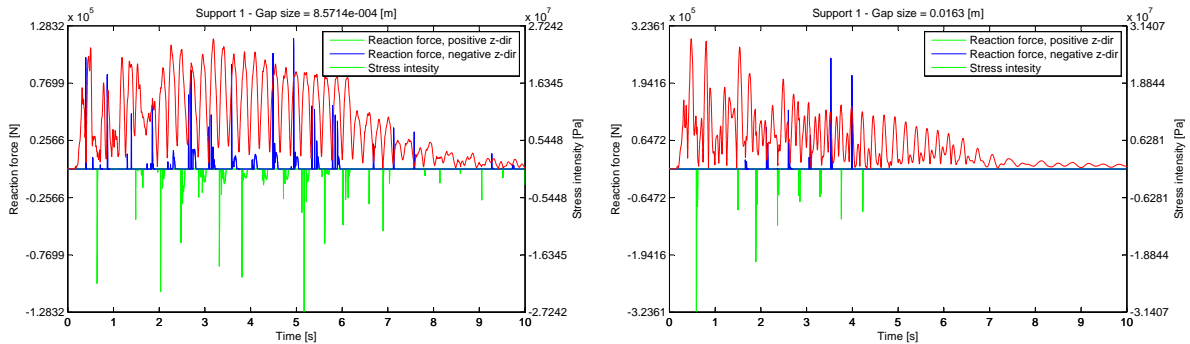Figure 4.33: Time history results for stress and reaction force at support A.

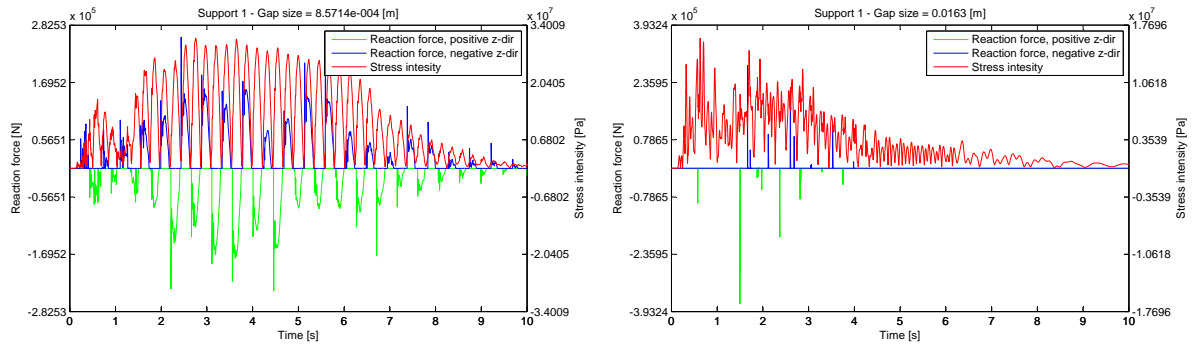Figure 4.34: Time history results for stress and reaction force at support B.

Figure 4.35: Time history results for stress and reaction force at support C.
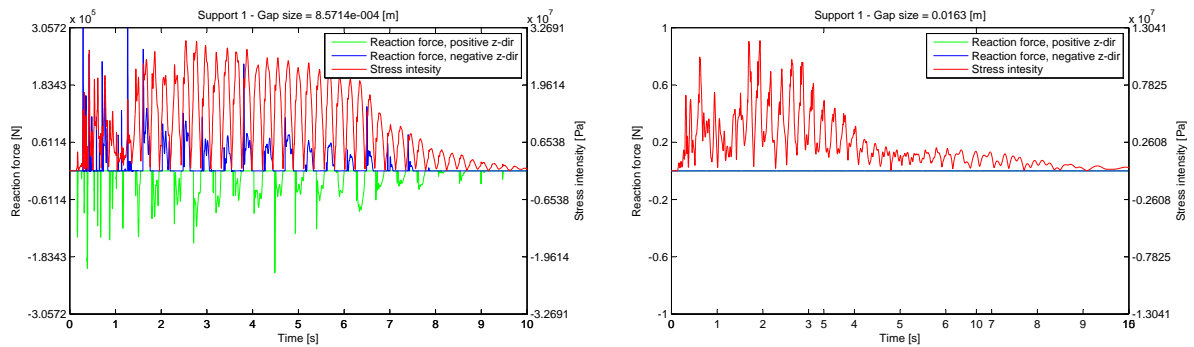

Figure 4.36: Time history results for stress and reaction force at support D.

In Figure 4.37 - 4.40 the results for gap sizes corresponding to the highlighted cases in Figure 4.31 are compared to the results for no gap. Standard support stiffness are used in all cases.
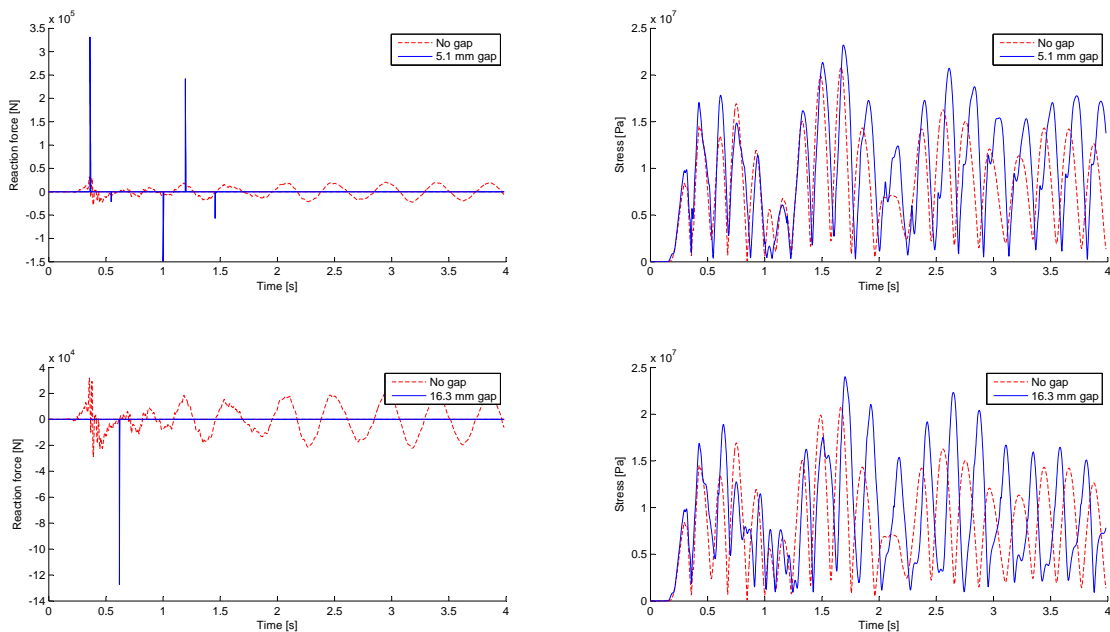

Figure 4.37: Time history results, stress and reaction force at support A, .
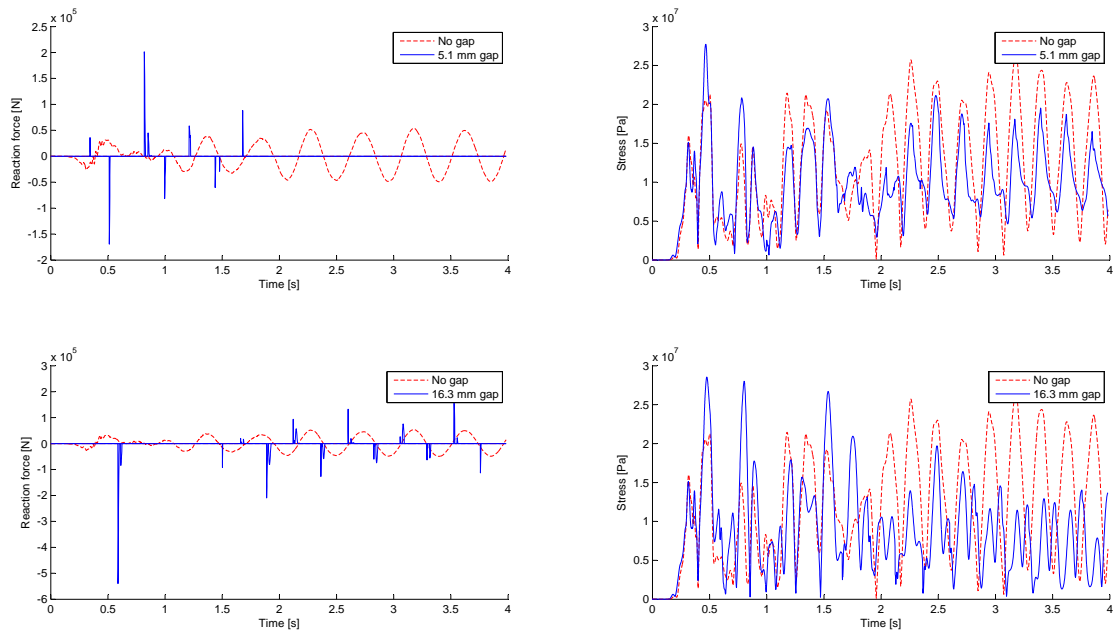
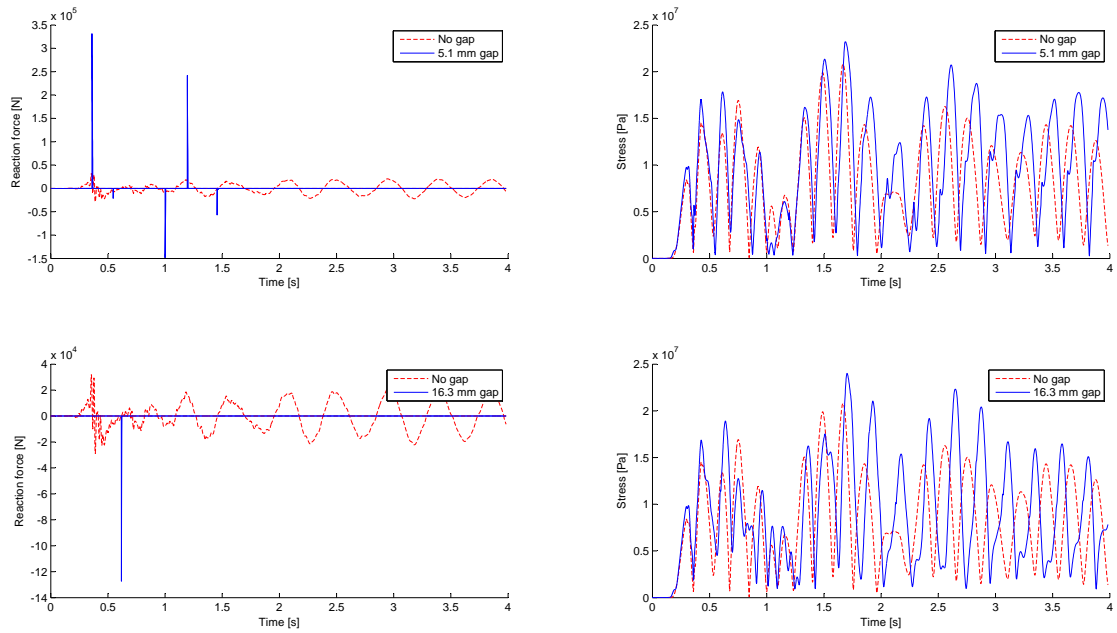Figure 4.38: Time history results for stress and reaction force at support B.

Figure 4.39: Time history results for stress and reaction force at support C.
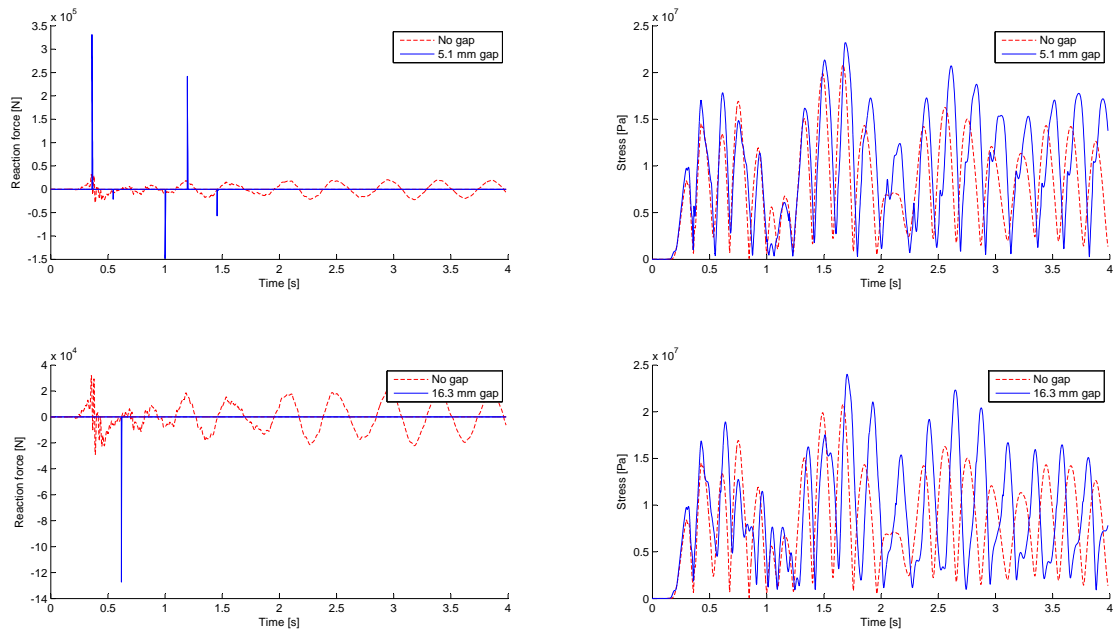
Figure 4.40: Time history results for stress and reaction force at support D.

4.3 Validation

After analyzing both the simplified piping system and the typical piping system in ANSYS and Pipestress with similar conditions, it was concluded that the two analyzes correlated. All validation parameters were compared and the differences were low. The only parameter that showed a noticeable difference was the element stresses from a pipe break analysis. These differences were due to different stress intensification factors in the bend and they were accounted for when the gap analysis results were post processed.

5 Conclusions and Discussion

In the time step analysis it appeared that it was very difficult to resolve the short duration reaction force that frequently appeared at first contact between the pipe and its supports. The amplitude of the reaction force spikes did not converge even if the time step was decreased until the practical limit for computational time. But on the other hand, if one instead considers the convergence of maximum stress in the pipe, it is more satisfying. The stress converges rapidly even at quite large time steps. If the characteristics of a time history element stress result is compared to a time history reaction force result, the similarities are striking, except on one point, the reaction force spikes.

Analysis was performed both with and without friction. Due to lengthy analyses, the number of gap sizes were limited. The selected set of gap sizes were chosen on the base of maximum support deformation. Despite the close connection between force and deflection it turned out that the support deformation did not show the same characteristic spikes as the reaction force, hence maximum support deformation was used when the gap sizes were chosen. The results, when friction in the contact between the pipe and its support were accounted for, indicate that the condition works satisfactory. For example, when comparing the displacement curves with and without friction, the energy loss from the pipe in the case of friction is noticeable. The general behavior of the pipe stresses is that they are lower when friction is accounted for due to energy loss. This indicates that it is a reasonable assumption to neglect friction in this kind of analysis.

The majority of all analyses performed in this thesis have been conducted using standard support stiffnesses, but due to the reaction force spikes and the question of how well it is possible to approximate a support gap with a spring, the influence of support stiffness has been investigated. First lets consider the relationship between support stiffness, when a gap exists, and reaction force spikes. When the support stiffness was lowered to one third of the standard stiffness, the spike characteristics disappeared due to lower acceleration in the impact. The other part of the reaction force, not the one associated with high acceleration immediately after impact but the long lasting one, is much less affected by the change in support stiffness. The computational time was decreased when weaker spring stiffnesses were used. This was in line with results reported in [14].

The essence of this thesis is the investigation regarding the influence of support gap size in a elastic piping systems. For example the question being raised in the introduction, weather it is conservative to neglect support gaps if the size is less then five millimeter? The analyses done on the geometry that was constructed to resemble a typical steam system indicate that it is not conservative to neglect gaps, with respect to reaction force, if the spikes were taken into account. Throughout this thesis, caution has been used when examining the force spike results. If the reaction force spikes are neglected, the results indicate that it is realistic assumption to neglect gap up to 5mm, both considering pipe stresses and support reaction forces.

How good is the correlation with larger gaps typically found in pipe break anchors for gaps larger than five millimeter? The simplified model shows results equally as for small gaps; if the spikes due to impact are neglected, one can neglect a support gap. In terms of stresses in the pipe system, it is even a slightly conservative approximation to neglect gaps. But if the spikes are considered, the maximum stress levels with a gap size equal to 20-40 millimeter increases with 20-30% in the studied simplified system and the reaction forces increases with up to 300%.

The simplified geometry analyzed indicates that both for small gaps, up to 5 mm, and gaps larger than 5 mm the approximation to neglect gaps gives best result if the support stiffness is equal in the approximative analysis as in the gap analysis, if the impact spikes are neglected. If the spikes are considered, it is possible that a lower spring stiffness is preferred due to its effect on the spike characteristic as previously mentioned.

During this thesis, many different contact elements were evaluated. In the final analysis, Conta178 was used to model the gap because of good setup options, possibility to model contact friction and possibilities to use different contact methods. However, the most straight forward contact element to work with was the Combin40 element. The downside to Combin40 is the lack of possible settings, for example the inability to choose contact method. Although, for faster analyses, it is a good alternative to Conta178.

6 Recommendations

For further work in this area we have the following recommendations:

- Use a elasto-plastic material model, in the contact surfaces and examine the plastic zone.

- Perform an explicit analysis to better resolve the fast contact forces that appear in gap support models. This could be done using, for example, LS-DYNA Explicit.

- Make a more detailed FEM model of the supports and pipe. Use smaller solid or shell elements instead of the pipe, beam elements, that were used in this thesis. This would lead to better knowledge about the stresses in the supports.

- Try to use a simpler load, for example, sinus shaped loads with different frequencies. This would give a better picture of how the results depend on the load case and its frequency range. By raising the the frequency of a half period sinus load, the effect of force spikes could also be investigated.

- The pipe break load in the simplified pinging system was calculated with steam as the fluid. Try a similar load with water as the fluid.

- Analyze a larger amount of pipe systems with different loads to get results that are reliable and to be able to make better conclusions.

- Try other kinds of supports with other kinds of stiffness nonlinearities. This thesis only considers rigid restrains. For example, a spring support that reaches maximum compression, with resulting stiffness increase, could be interesting.

- Investigate if there is a more realistic way to model the damping. A Rayleigh damping, approximated to reassemble a constant damping of 5% may not be optimal from this point of view.

References

[1] Ansys. http://www.ansys.com.

[2] Ansys release 11.0 documentation for ansys. http://www.ansys.com.

[3] Asme. http://www.asme.net.

[4] Pipestress. http://www.dst.ch/.

[5] Asme section iii, rules of nuclear power plant components, division 1 - subsection nc, article nf-1000, nc-1132. http://www.asme.net, 1995.

[6] Asme section ii,rules of nuclear power plant components, part d. http://www.asme.net, 2003.

[7] Klaus-Jurgen Bathe. *Finite Element Procedures in Engineering Analysis.* Prentice-Hall,Englewood Cliffs, New Jersey, 1982.

[8] Javier Bonet and Richard D. Wood. *Nonlinear Continuum Mechanics for Finite Element Analysis 2nd edition.* Cambridge University Press, 2008.

[9] David Hutton. *Fundamentals of Finite Element Analysis.* The McGraw Hill Companies, Washington, 2004.

[10] Benjamin R. STRONG Jr. and Ronald J. BASCHIERE. *Pipe rupture and steam/water hammer design loads for dynamic analysis of piping systems.* Advanced Analysis Division, EDS Nuclear Inc., San Francisco, 1977.

[11] Igli Micheli and Piero Zanaboni. An analytical validation of simplified methods for the assessment of pipe whip characteristics, 2003.

[12] Niels Ottosen and Hans Petersson. *Introduction to the Finite Element Method.* Prentice Hall Europe, 1992.

[13] Paul R. Smith and Thomas J. Van Laan. *Piping and pipe support systems: design and engineering.* McGraw Hill Book Co.,New York, NY, 1987.

[14] Hsiang-Chuan Tsai and Ming-Kuen Wu. *Methods to compute dynamic response of cantilever with a stop to limit motion.* Department of Construction Engineering, National Taiwan Institute of Technology, Tapei, 1994.

[15] Jr. William Weaver and James M. Gere. *Matrix Analysis Of Framed Structures, 3rd Edition.* Springer-Verlag New York, LLC, 1966.

[16] Peter Wriggers. *Computational contact mechanics, second edition.* Springer, Berlin Heidelberg New York, 2006.

[17] Peter Wriggers. *Nonlinear Finite Element Methods.* Springer, Berlin Heidelberg, 2008.

A   Simplified piping system, time history force

In this Appendix the resulting time history force components from the pipe break in $geom1\_v_1 - geom1\_v_4$ are shown in the figures below.
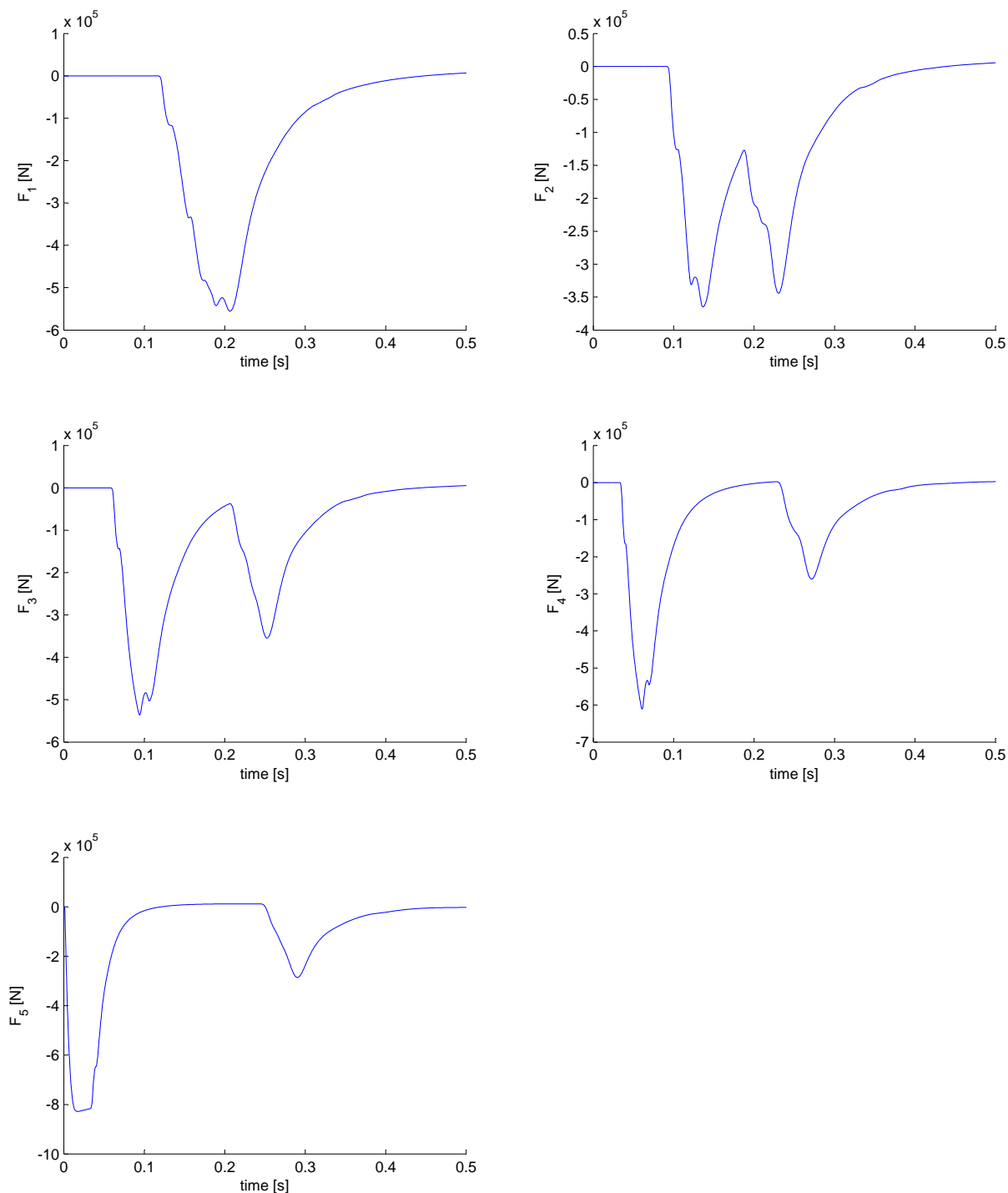

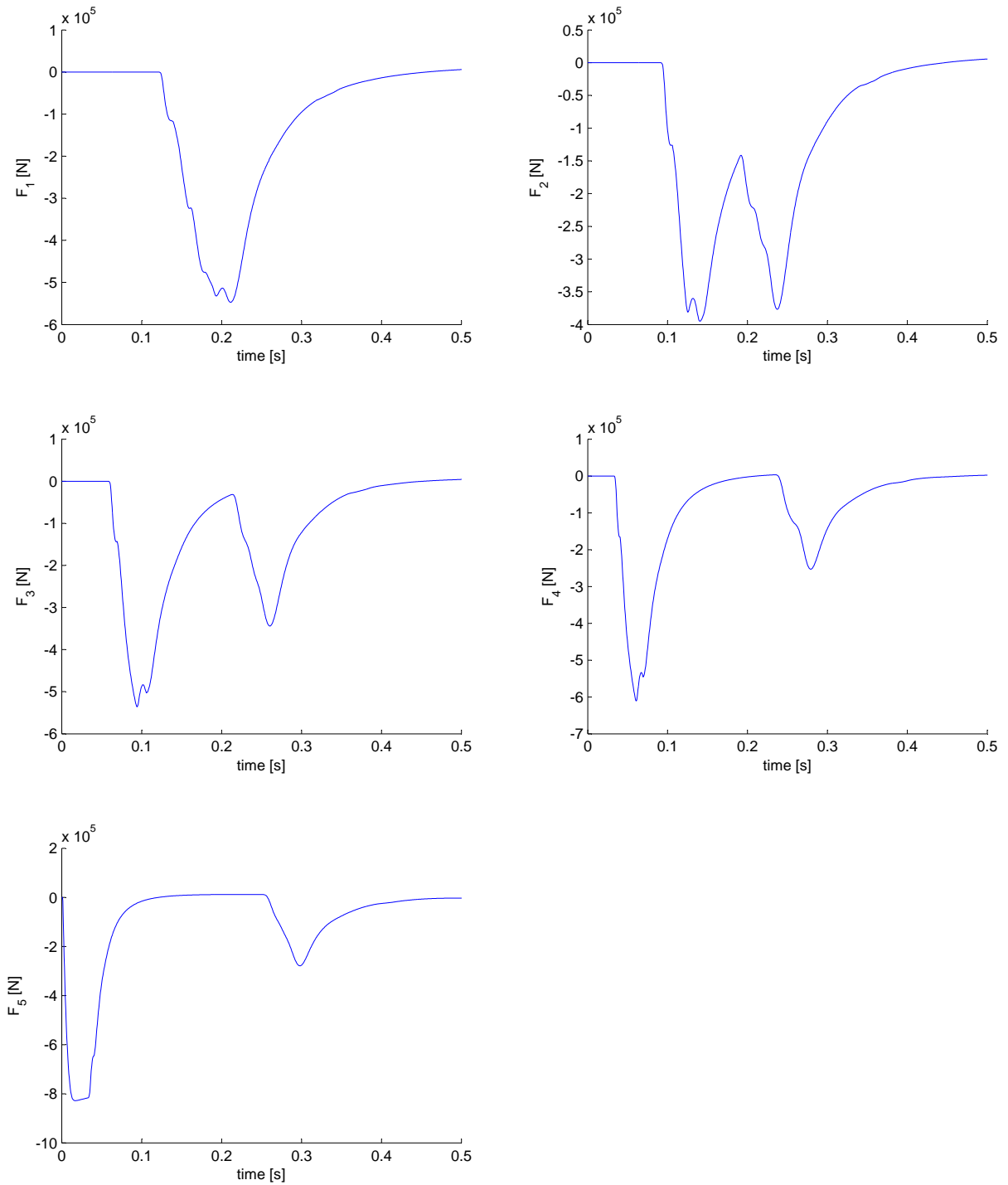Figure A.1: Time history force components of $geom1\_v_1$.
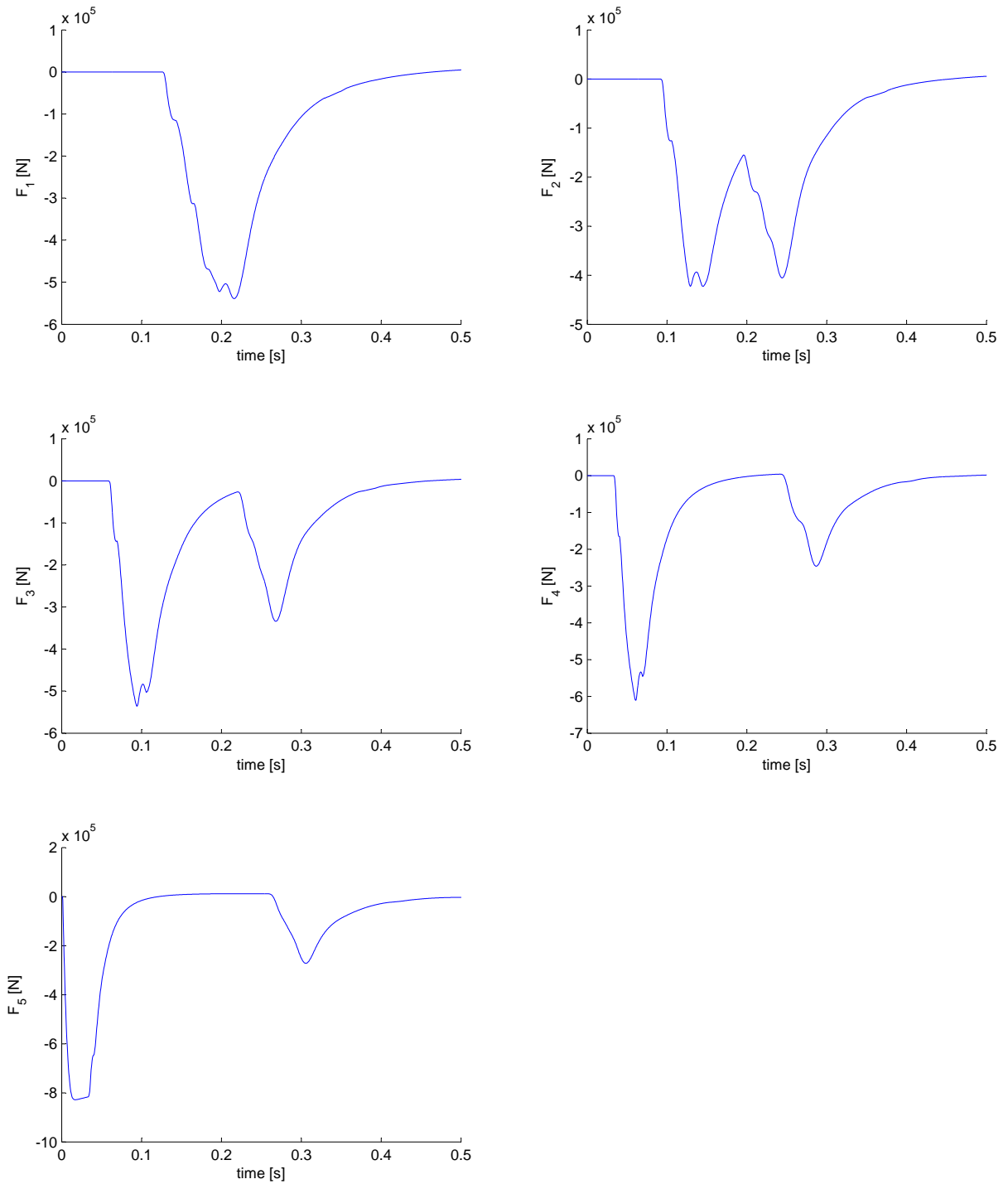
Figure A.2: Time history force components of *geom*1_v_2.

CHALMERS, *Applied Mechanics*, Master's Thesis 2011:32

Figure A.3: Time history force components of *geom*1_*v*₃.
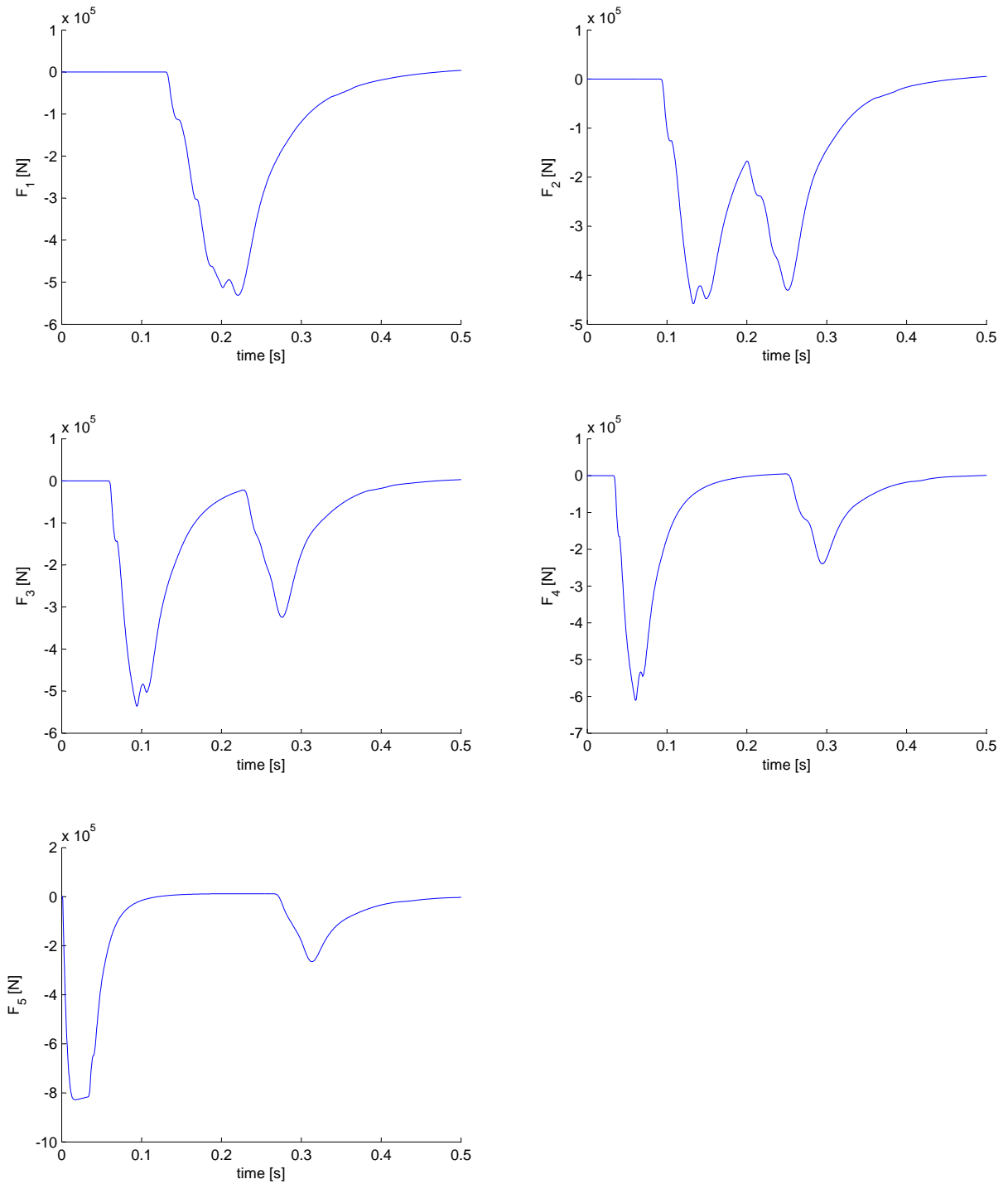
Figure A.4: Time history force components of $geom1\_v_4$.

B Simplified piping system, time history force

This Appendix contains the resulting time history force components from the pipe break in the typical piping system. The figures show the resulting absolute forces of the x,y and z components in nine points of the pipe.
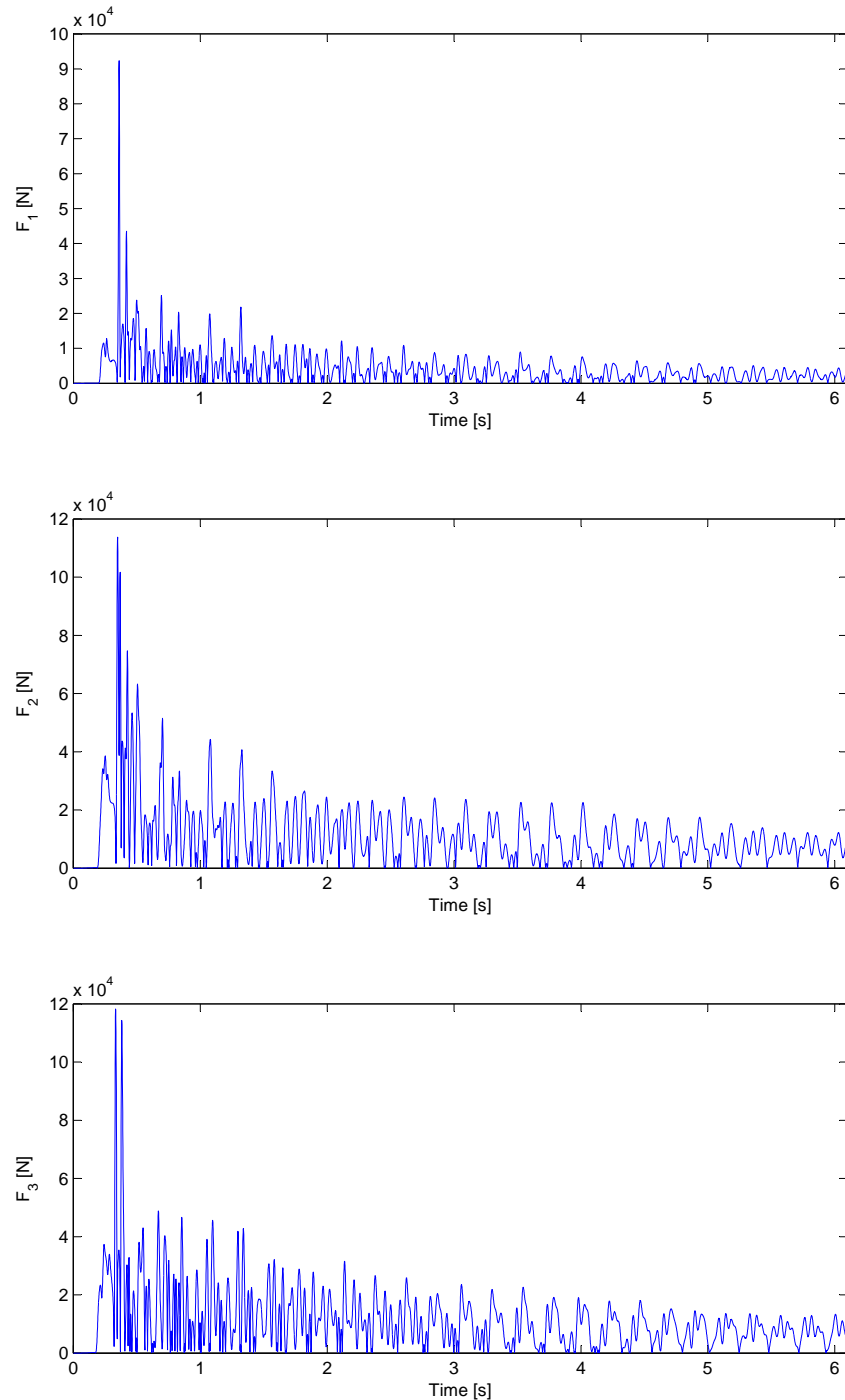

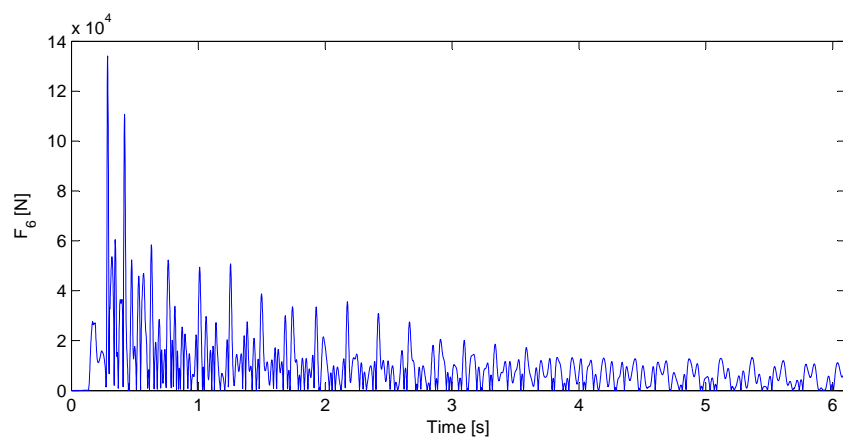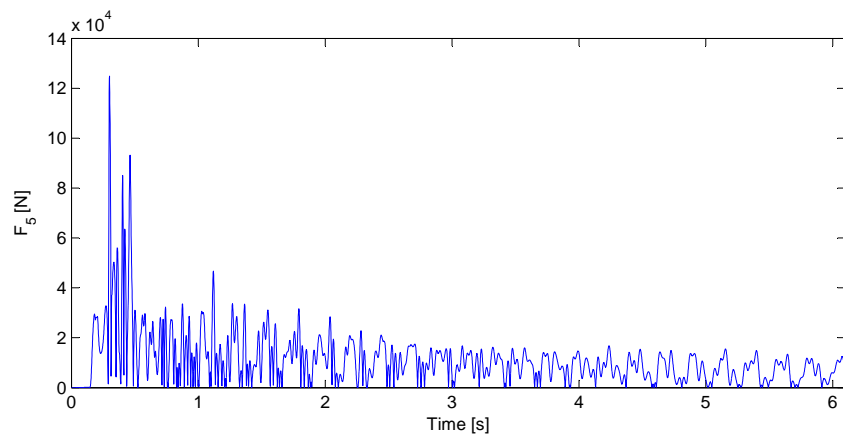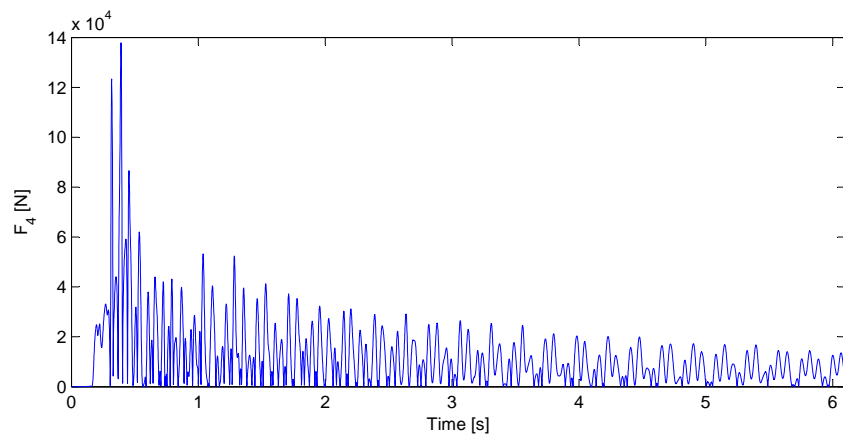Figure B.1: Time history force components of the typical piping system, F_1-F_3

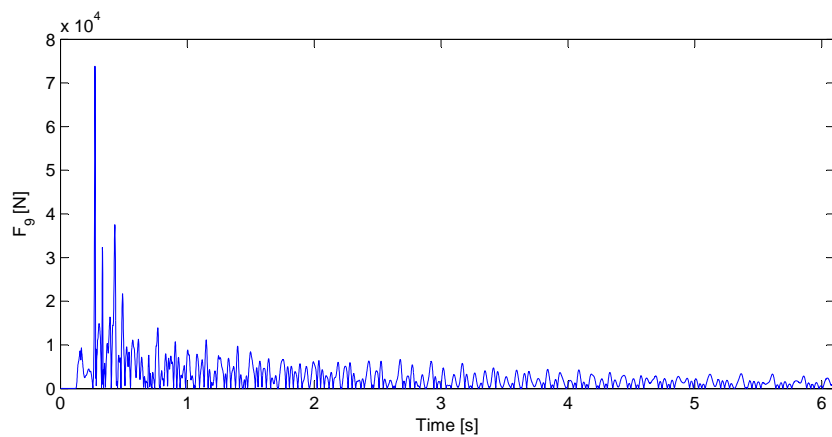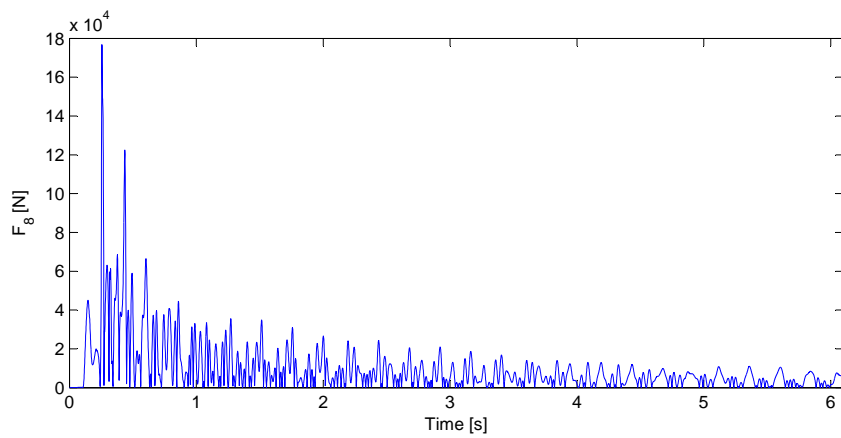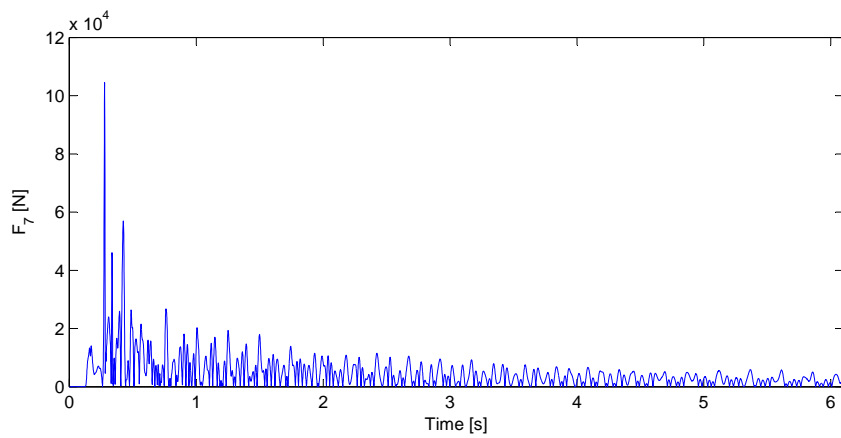Figure B.2: Time history force components of the typical piping system, F_4-F_6

Figure B.3: Time history force components of the typical piping system, F_7-F_9

C Standard support stiffness

The table below includes generally accepted standard support stiffnesses from the Swedish nuclear power plant industry.

Rördimension	Ytterdiameter mm	Godstjocklek mm	Vikt kg	BESKRIVNING	Cr KN/mm	KX,KY,KZ KZ KN/mm	MX,MY,MZ MZ kN·m/rad
30" Sch 5S	762.00	6.35	118.3	30" Sch Std infinite	560	560	560.E3
30" Sch 10 10S	762.00	7.92	147.3	30" Sch Std standard	210	210	210.E3
30" Sch Std	762.00	9.52	176.7	30" Sch 20 infinite	900	900	9.E5
30" Sch 20 XS	762.00	12.70	234.7	30" Sch 20 standard	330	330	330.E3
30" Sch 30	762.00	15.87	292.0	30" 1" WT infinite	1500	1500	1.5E6
				30" 1" WT standard	600	600	6.E5
				30" 1.25" WT infinite	1900	1900	1.9E6
				30" 1.25" WT standard	700	1901	7.E5